Journal of Agriculture and Food Research 26 (2026) 102726

Contents lists available at ScienceDirect

Journal of Agriculture and Food Research

journal homepage: www.sciencedirect.com/journal/journal-of-agriculture-and-food-research

Occurrence, sources, and ecological risk of polycyclic aromatic hydrocarbons (PAHs) in rice field soils of northwestern Peru☆

Cristian Culqui [a,b], Daniel Tineo [b,*], Jorge A. Fernández-Jibaja [b], Yeltsin A. Álvarez-Robledo [b], Larry D. Garcia-Frias [b], Jani Mendoza-Merino [c], Victor H. Taboada-Mitma [b], Juancarlos Cruz-Luis [d], Nilton B. Rojas-Briceño [e], Ligia García [f,g], Franz Zirena Vilca [h], Malluri Goñas [b]

[a] Escuela de Posgrado, Maestría en Cambio Climático Agricultura y Desarrollo Rural Sostenible MACCARD, Universidad Nacional Toribio Rodríguez de Mendoza de Amazonas, Chachapoyas, 01001, Peru
[b] Centro Experimental Yanayacu, Dirección de Servicios Estratégicos Agrarios (DSEA), Instituto Nacional de Innovación Agraria (INIA), Carretera Jaén San Ignacio KM 23.7, Jaén, 06801, Peru
[c] Universidad Nacional Mayor de San Marcos, Programa de Doctorado en Ciencias Biológicas, Lima, Peru
[d] Dirección de Servicios Estratégicos Agrarios (DSEA), Instituto Nacional de Innovación Agraria (INIA), Av. La Molina 1981, Lima, 15024, Peru
[e] Grupo de Investigación en Ciencia de la Información Geoespacial, Escuela Profesional de Ingeniería Ambiental, Facultad de Ingenierías, Universidad Nacional de Moquegua, Pacocha, 18610, Peru
[f] Instituto de Investigación para el Desarrollo Sustentable de Ceja de Selva, Universidad Nacional Toribio Rodríguez de Mendoza de Amazonas, Chachapoyas, 01001, Peru
[g] Facultad de Ingeniería Zootecnista, Agronegocios y Biotecnología, Universidad Nacional Toribio Rodríguez de Mendoza de Amazonas, Chachapoyas, Peru
[h] Laboratory of Organic Pollutants and Environment of the IINDEP of the Universidad Nacional de Moquegua, Urb Ciudad Jardín-Pacocha-Ilo, Moquegua, Peru

ARTICLE INFO

Keywords:
Persistent organic pollutants
Soil contamination
Agricultural soil degradation
Polycyclic aromatic hydrocarbons (PAHs)
UHPLC-FLD

ABSTRACT

Polycyclic aromatic hydrocarbons (PAHs) are organic contaminants that pose significant risks to human health and ecosystems. This study investigated the occurrence, sources, and ecological risks of PAHs in rice paddy soils from northwestern Peru. Ninety-seven soil samples were collected at a depth of 30 cm across three altitudinal zones, four phenological stages, and two agronomic management practices. Quantification was performed using ultra-high-performance liquid chromatography coupled with fluorescence detection (UHPLC-FLD). Source apportionment was conducted through rotated principal component analysis combined with multiple linear regression. Ecological risk was assessed using organic carbon normalization and the mean effects range-median quotient (M-ERM-Q) method, while carcinogenic potential was estimated using the toxic equivalent factor (TEQ_{CARC}). Total PAHs ranged from 22.02 to 130.55 ng g^{-1} (mean: 55.26 ng g^{-1}); LMW PAHs averaged 37.38 ng g^{-1}, exceeding HMW PAHs (17.88 ng g^{-1}). No significant differences were observed among altitudinal zones, phenological stages or agronomic practices ($p > 0.05$). The predominant sources of PAHs were attributed to vehicular emissions (52.3%), petroleum and biomass combustion (42.1%), and coal combustion (5.4%). Ecological risk assessment revealed low contamination levels below established safety thresholds (CEC <290 μg g^{-1}), consistent with the carcinogenic risk estimated through TEQ_{CARC} (0.0083 to 18.7483 ng BaP_{eq} g^{-1}). This study provides the first comprehensive evaluation of PAHs contamination in rice paddy soils in Peru and underscores the influence of altitude and agricultural practices, emphasizing the need for further research on pollution sources, impacts on crop productivity, and potential risks to human health.

☆ This study was funded by Investment Project with CUI No 2472675: "Mejoramiento de los servicios de investigación y transferencia de tecnología agraria en la estación agraria experimental Baños del Inca en la localidad de Baños del Inca del distrito de Baños del Inca - provincia de Cajamarca - departamento de Cajamarca", Dirección de Servicios Estratégicos Agrarios (DSEA), Instituto Nacional de Innovación Agraria (INIA).

* Corresponding author.
E-mail address: dt.infolab@gmail.com (D. Tineo).

https://doi.org/10.1016/j.jafr.2026.102726
Received 21 October 2025; Received in revised form 20 January 2026; Accepted 27 January 2026
Available online 4 February 2026

1. Introducción

Rice (*Oryza sativa* L.) is one of the most significant cereal crops globally, ranking third in total production after maize and wheat, and serving as the primary dietary staple for over 60% of the world's population [1,2]. Approximately 90% of both rice production and consumption occur in Asia, where China and India are the leading producers [3]. In Latin America and the Caribbean, rice constitutes the main source of carbohydrates for human consumption [4], with Brazil being the largest producer, reaching a production of 10,671,490 tons in 2024 [5]. In Peru, rice cultivation covers more than 400,000 ha, with an estimated production of two million tons projected for 2025 [6]. Within the province of Jaén, located in the Cajamarca region of northwestern Peru, rice contributes 29.7% to the provincial gross production value (GPV), engaging 4610 producers who collectively manage 14,592 ha; among the principal producing districts, Bellavista and Jaén reported the highest outputs, reaching 8709.10 tons in 2024 [7].

Conversely, global rice demand continues to increase, and projections indicate that by 2050, production will need to rise by approximately 70% to sustain a population expected to reach 9.7 billion [8–10]. In response to this growing demand, farmers have adopted intensive agricultural practices aimed at maximizing yields while minimizing production costs. However, inadequate agronomic management, such as post-harvest residue burning and irrigation with untreated wastewater, contributes to the generation and accumulation of toxic pollutants, including polycyclic aromatic hydrocarbons (PAHs) [11–14], which are persistent organic compounds known for their deleterious effects on both human health and the environment [15].

PAHs are organic compounds composed of two or more fused benzene rings, originating from both natural sources such as volcanic eruptions, forest fires, and the weathering of oil-bearing rock formations [16–18] and anthropogenic activities, including incomplete combustion, pyrolysis of organic matter, and fossil fuel burning [19–23]. Pyrogenic sources are characterized by a predominance of high-molecular-weight (HMW) PAHs, whereas petrogenic sources are mainly composed of low-molecular-weight (LMW) PAHs [24]. These sources can be determined using principal component analysis combined with multiple linear regression (PCA-MLR), enabling the identification of the activities that contribute most substantially within the assessed environment [13,25,26]. PAHs tend to accumulate and be transported through soil, water, and air [27–30], and can be readily absorbed by plants, where they accumulate in roots, stems, leaves, and grains [28,31]. Their mobility through the food chain, together with their persistence and environmental recirculation, poses substantial ecological and carcinogenic risks to humans. Due to their persistence and toxicity, several international frameworks and monitoring programs have been implemented to regulate PAHs contamination in agricultural systems [32].

Several studies have reported the occurrence of PAHs in multiple environmental matrices, including water, soil, and air [20,32–35]. The accumulation of these compounds in soil can reduce the abundance and diversity of microbial communities [36], and can also impair plant growth and development [37] and may disrupt soil microbiota, thereby altering ecological dynamics [38]. Ecological risks associated with PAHs have been assessed using various approaches, including organic carbon normalization [13,22] and the mean effects range–median quotient (M-ERM-Q) [33,35,39,40], which enable the classification of areas according to toxicity levels. In particular, M-ERM-Q is used as a regulatory benchmark by the Canadian Council of Ministers of the Environment [41], and is implemented under Peruvian regulations [42]. Moreover, the accumulation of PAHs has been confirmed in the tissues of rice and wheat plants [28,31,32], and substantial evidence demonstrates that PAHs possess toxic, mutagenic, and carcinogenic properties, being linked to lung and esophageal cancers, as well as cardiovascular and respiratory disorders [43,44]. To evaluate carcinogenic risk from PAHs, toxic equivalency factors (TEFs) are commonly applied [45], and cancer risks associated with daily rice consumption have been reported in the major rice-growing regions of China [14]. Collectively, these findings highlight the global concern regarding PAHs in food crops and underscore the importance of monitoring their presence in staple cereals such as rice [28,31,32].

In Peru, studies addressing PAHs remain limited, with existing research primarily focused on soils from mining [46], fishing [47], and urban areas [48], as well as on soils affected by intentional grassland burning [49]. However, despite their economic importance to national food security, this knowledge gap represents a fundamental limitation in understanding the potential risks to consumers and ecosystems [50]. Therefore, this study aimed to assess the presence and spatial distribution of PAHs in rice-growing areas of Jaén, Peru, to identify their potential sources and to estimate associated ecological and carcinogenic risks. To achieve this, different phenological stages of rice and local agricultural management practices such as stubble burning and soil fallowing were considered, in order to provide scientific evidence that supports the monitoring and control of these contaminants. In this study, we propose that altitude, the agricultural practice of burning, proximity to urban areas, and wastewater treatment plants would affect PAH concentrations in rice-growing areas.

2. Material and methods

2.1. Study area

The study area comprises agricultural land located in the lower section of the Amojú River basin, partially encompassing the districts of Jaén and Bellavista. Both districts belong to the province of Jaén, Cajamarca region, Peru (Fig. 1). The region is characterized by maximum temperatures ranging from 29 °C to 33 °C and minimum temperatures between 19 °C and 23 °C, with an estimated annual precipitation of 900-1200 mm [51].

2.2. Sample collection

The agricultural land map and a regular 1 km grid were used as the basis for locating sampling points, resulting in a total of 97 soil samples collected from rice fields. All soil samples were collected in June 2024, corresponding to the rainy season; a single core was taken at each sampling point following the sampling procedure described by Ref. [20], with the exception that samples were collected from the 0–30 cm soil layer to capture the zone with the highest root density in flooded systems [52]. Soil physicochemical properties are summarized in Table 1. A spiral auger with a 2.5 cm diameter was used to collect approximately 1 kg of soil at each point. Each sample was transferred in a plastic bag and labeled according to the phenological stage of the crop (seedling, tillering, filling, and ripening) and the agronomic management practice (fallow or burning) applied at the time of collection (Fig. 1). The samples were then transported to the Soil, Water, and Foliar Laboratory of the Yanayacu Experimental Center, where they were air-dried, gently crushed, and sieved through a 0.25 mm mesh. Finally, 500 g of each sample was subsampled and stored at 4 °C until analysis.

2.3. Identification and quantification of PAHs

2.3.1. Analysis and quantification of PAHs

For the analysis, fifteen PAHs were considered: naphthalene (Nap), Acenaphthylene (Acy), fluorene (Flu), phenanthrene (Phe), anthracene (Ant), fluoranthene (Flt), pyrene (Pyr), benzo[a]anthracene (BaA), chrysene (Chr), benzo(b)fluoranthene (BbF), benzo(k)fluoranthene (BkF), benzo(a)pyrene (BaP), dibenzo[a,h]anthracene (DahA), benzo(g,h,i)perylene (BghiP), and indeno(1,2,3-cd)pyrene (IcdP). PAHs was performed using ultra-high-performance liquid chromatography (UHPLC, Agilent 1290 Infinity II) coupled with a fluorescence detector (FLD), following the protocol developed at the Laboratory of Organic

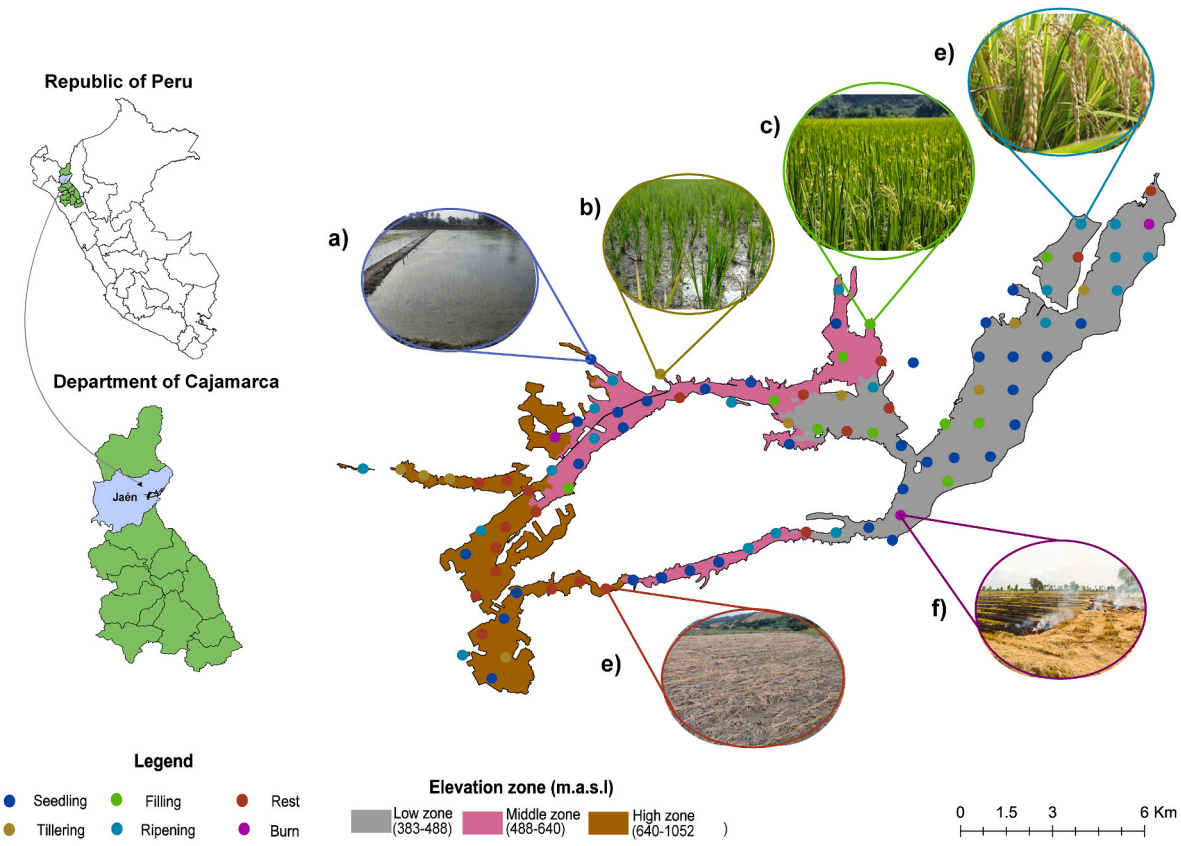

Fig. 1. The map illustrates the study area and sampling points with regard to their geographic location. The software was developed using ArcGIS Pro v3.1.0 software, which can be accessed at https://pro.arcgis.com/es/pro-app/latest/get-started/install-and-sign-in-to-arcgis-pro.htm. The altitude classification was generated from a digital elevation model (DEM) downloaded from ASF Data Search Vertex, https://search.asf.alaska.edu.

Table 1
Soil properties in rice-growing areas of Jaén, Peru.

Soil properties	Unit	Mean	Median	Std	Range
pH	pH unit	7.64	7.80	0.60	5.300 – 8.700
Electrical conductivity	mSm^{-1}	26.78	21.80	19.06	7.500 – 146.300
Organic matter	%	1.96	1.90	0.60	0.900 – 3.900
Organic carbon	mg kg^{-1}	11,351.73	10,986.00	3505.53	5076.000 – 22,666.000
Available phosphorus	mg kg^{-1}	13.32	11.00	7.71	4.4000 – 65.5000
Sand	%	40.99	40.50	13.30	16.6000 – 75.4000
Clay	%	29.97	30.10	8.98	8.7000 – 51.8000
Silt	%	29.02	28.00	8.83	9.4000 – 55.9000

Contaminants and Environment, National University of Moquegua [49].

Compound separation was achieved using an Agilent ZORBAX Eclipse PAHs analytical column maintained at 25 °C. A 10 μL aliquot of each sample was injected, with a mobile-phase flow rate of 1.8 mL min^{-1}. Elution was carried out using a gradient of water and Acetonitrile under varying time intervals. To ensure analytical accuracy and precision, certified reference standards (500 μg mL^{-1}; Agilent; purity >99%) were used. A mixed stock solution containing the 16 PAHs was prepared at 50 μg mL^{-1} by dilution in acetonitrile. Working calibration solutions were then prepared at five concentration levels (0.005, 0.05, 0.1, 0.2, and 0.5 μg mL^{-1}) for instrument calibration and method validation. Both positive and negative controls were employed. The identification and quantification of each PAHs were based on their characteristic excitation and emission wavelengths recorded by the fluorescence detector (Table 2). PAHs were validated based on the limit of detection (LOD), limit of quantification (LOQ), recovery percentage (Table S1), and abbreviation (Abbr.), Molecular Weight (MW, g/mole), number of rings, TEF (toxic equivalent factor) [1], ERM (effects range median value) (Table S2).

To contextualize the results, PAHs were descriptively analyzed on an individual basis, using the total sum of PAHs, the sum of low-molecular-weight PAHs (LMW PAHs), and the sum of high-molecular-weight PAHs (HMW PAHs). For each case, the mean, median, standard deviation, value range, and detection frequency (both absolute counts and percentages) were reported. LMW PAHs (2–3 aromatic rings) include Nap, Ace, Flu, Phe, and Ant, whereas HMW PAHs (4–6 aromatic rings) include Flt, Pyr, BaA, Chr, BbF, BkF, BaP, DahA, BghiP, and Ind.

2.3.2. Comparison of PAHs concentration by altitude zone

The shapefile of the agricultural area of Jaén Province [53] and an ALOS PALSAR Digital Elevation Model (DEM) with a spatial resolution of 12.5 m [54] were obtained for spatial analysis. In ArcGIS Pro v3.1.0, the DEM was clipped using the Extract by Mask tool based on the agricultural area shapefile. The study area was subsequently divided into three altitudinal zones using the Reclassify tool: low (383-488 m a.s.l.), middle (488-640 m a.s.l.), and high (640-1052 m a.s.l.). The sampling

Table 2
Analytical conditions for UHPLC-FLD detection of PAHs.

Chromatographic conditions			
Parameter	Value		
Analytical column	Agilent ZORBAX Eclipse PAHs 4.6 i.d. x 100 mm, 1.8 μm		
Column temperature	25 °C		
Injection volume	10 μL		
flow	1,8 mL min^{-1}		
Mobile phase	Time (min)	Water (%)	Acytonitrile (%)
	0	55	45
	6	0	100
	9.5	0	100
	10	55	45
FLD conditions	Time (min)	Emission (mm)	Excitation (mm)
	2.97	314	210
	3.40	3.14	210
	3.80	3.68	250
	4.40	402	252
	4.57	402	252
	4.79	440	237
	5.20	420	255
	5.60	420	255
	6.90	453	234
	8.00	453	234
	8.90	453	234

point database was incorporated into the GIS environment to generate a point shapefile. The Spatial Join tool was applied to assign each sampling point to its respective elevation category. The processed dataset was then exported and analyzed in the Google Colaboratory environment using the NumPy, Pandas, Seaborn, and Matplotlib libraries to visualize the spatial distribution and mean concentrations of PAHs across altitude ranges. Finally, the nonparametric Kruskal-Wallis test was employed to evaluate significant differences among the altitudinal zones.

2.3.3. Comparison of PAHs across phenological phases and agronomic practices

To compare PAHs concentrations across crop phenological stages and agronomic management practices, the sum of the mean concentrations of individual PAHs was evaluated. The nonparametric Kruskal Wallis test was employed to assess significant differences in PAHs concentrations among phenological stages and management practices. Additionally, principal component analysis (PCA) was conducted to identify groupings of phenological stages and agronomic practices based on their PAHs composition patterns. Finally, 95% confidence ellipses were incorporated to enhance the interpretation of multivariate relationships.

2.4. Identification of potential sources of PAHs origin

The diagnostic ratios [Flt/(Flt + Pyr)] vs [Ind/(Ind + BghiP)] [55] and [Flt/(Flt + Pyr)] vs. [Ant/(Ant + Phe)] [56] were used to distinguish between pyrogenic and petrogenic sources of PAHs. The classification thresholds were as follows: 1) Flt/(Flt + Pyr) < 0.40 (petrogenic), 0.40–0.50 (petroleum combustion), and >0.50 (biomass/coal combustion); 2) Ind/(Ind + BghiP) < 0.20 (petrogenic), 0.20–0.50 (petroleum combustion), and >0.50 (biomass/coal combustion) [46]; and 3) Ant/(Ant + Phe) < 0.10 (petrogenic) versus >0.10 (combustion) [56]. Source contribution quantification was performed using the Principal Component Analysis-Multilinear Regression (PCA-MLR) approach described by Wang et al. [57], In this framework, potential sources are inferred by interpreting the Varimax-rotated component loadings and comparing them with characteristic PAH fingerprints reported in the literature. The suitability of the dataset for PCA was assessed using the Kaiser Meyer Olkin (KMO ≥0.60) measure of sampling adequacy and Bartlett's test of sphericity ($p < 0.05$) [13,58], confirming that the correlation structure was appropriate for factor extraction. Upon meeting these assumptions, PCA was performed on standardized variables, and varimax orthogonal rotation was applied to enhance interpretability by achieving a simpler loading structure. Horn's parallel analysis (95th percentile) was used to determine the number of components to retain, resulting in three principal components (PC1, PC2, and PC3) that explained a moderate proportion of the total variance. The rotated component scores of the Varimax-rotated components (RC1, RC2 and RC3) were used as independent variables in an multiple linear regression model, with ΣPAHs as the dependent variable (Equation (1)). Source contribution ratios were quantified using the absolute standardized regression coefficients (|β*|), expressed as fractional percentages of the total absolute standardized effect across components. To address heteroscedasticity, we used robust standard errors (HC3). Rotated loadings are presented as absolute values for visualization, whereas rotated component scores were used with their original sign in the MLR.

$$\sum HAPs = \beta 0 + \beta 1\ RC1 + \beta 2\ RC2 + \beta 3\ RC3 + \varepsilon \quad \text{(Equation 1)}$$

Where: $\Sigma PAHs$ is the sum of PAH concentrations, $\beta 0$ is the intercept, $\beta 1 - \beta 3$ are the regression coefficients, $RC1–RC3$ are the Varimax-rotated component scores, and ε is the random error term.

2.5. Assessment of ecological risk and carcinogenic potential

The carbon normalization methodology described by Ref. [13] was applied, excluding Acynaphthylene (Acy), which was not evaluated in this study. The procedure involved comparing the sum of 12 PAHs (Nap, Ace, Flu, Phe, Ant, Pyr, Baa, Chr, Bbf, Bkf, Bap) against established threshold values: critical effect concentration (CEC = 290 μg g^{-1}), mean effect concentration (MEC = 1800 μg g^{-1}), and extreme effect concentration (EEC = 10,000 μg g^{-1}) [59]. An organic carbon–normalized criterion was applied because ecological risk varies with the amount of organic carbon present in the soil. The organic carbon normalization procedure was applied to account for differences in soil organic carbon that may influence PAH sorption and, consequently, ecological risk. In this approach, OC (mg kg^{-1}) was first converted to an organic-carbon fraction f_{OC} (Equation (2)), and $\Sigma PAHs$ (ng g^{-1} dry soil) was then normalized by dividing $\Sigma PAHs_{soil}$ by f_{oc} to obtain $\Sigma PAHs_{oc}$ in ng g^{-1} OC (Equation (3)). Finally, $\Sigma PAHs_{oc}$ was re-expressed in μ g g^{-1} OC to ensure consistency with the reference framework (Equation (4)).

$$f_{OC} = \frac{OC\ (mg\ kg^{-1})}{10^6} \quad \text{(Equation 2)}$$

$$\Sigma PAHs_{OC} = \frac{\Sigma PAHs_{soil}}{f_{OC}} \quad \text{(Equation 3)}$$

$$\Sigma PAHs_{OC}\ (\mu g\ g^{-1}\ OC) = \frac{\Sigma PAHs_{OC}\ (ng\ g^{-1}\ OC)}{10^3} \quad \text{(Equation 4)}$$

Where: OC is the soil organic carbon content, f_{OC} is the organic-carbon fraction, $\Sigma PAHs_{soil}$ is the summed PAH concentration on a dry-soil basis (ng g^{-1}), and $\Sigma PAHs_{OC}$ is the carbon-normalized summed PAH concentration (ng g^{-1} OC or mg g^{-1} OC).

Similarly, the mean effects range-median quotient (M-ERM-Q) method (Equation (5)) was applied to assess ecological risk, considering risk categories classified as low (<0.1), medium-low (0.11-0.50), medium-high (0.51-1.50), and high (>1.50) [58].

$$M - ERM - Q = \frac{\sum Ci/ERM_i}{n} \quad \text{(Equation 5)}$$

Where: "Ci" represents the concentration of the individual PAHs in the soil, "ERM_i" denotes the ERM value of the individual PAHs, and "n" is the total number of PAHs. The corresponding ERM values for each PAHs are listed in Table fig.

To evaluate the potential of PAHs to induce DNA (deoxyribonucleic acid) alterations and assess their genotoxicity, the BaP equivalent factor

(BaP_eq) approach (Equation (6)) was applied [15]. Carcinogenic risk levels were categorized as follows: no risk (<0.1), low risk (0.1-1), low to moderate risk (1-10), moderate to high risk (10-100), and high risk (≥100). Additionally, the Peruvian Environmental Quality Standards (ECA) for soil [42] were considered, adopting the Canadian Soil Environmental Quality Guideline (600 ng g^{-1}) [41] as the reference threshold.

$$TEQ^{carc} = \sum_i C_i \times TEF_i^{carc} \quad \text{(Equation 6)}$$

Where: TEQ^{carc} is the BaP equivalent factor; Ci is the mean concentration of each PAHs expressed in nanograms per gram (ng g^{-1}); and TEF_i^{carc} is the toxic equivalency factor relative to BaP [45].

To spatially represent ecological risk levels and carcinogenic potential, the Kriging interpolation method was applied in ArcMap 10.8 after fitting the experimental semivariogram. The model's performance and suitability were evaluated through cross-validation, which yielded a bias near zero, a minimal root mean square error (RMSE), and a ratio of partial least squares (PLS) error to variance close to 1, consistent with the validation criteria described in Ref. [60] Zonal classification was performed using the thresholds defined in the methodology. However, when values did not exceed those thresholds, we applied the Natural Breaks (Jenks) criterion in ArcGIS Pro to classify the areas, prioritizing the identification and visualization of the main PAH influence hotspots and highlighting natural shifts in the distribution of values.

2.6. Statistical analysis

Statistical analyses were conducted to evaluate differences in polycyclic aromatic hydrocarbon (PAH) concentrations among altitudinal zones, phenological stages, and agronomic management practices. Because the dataset did not meet the assumptions of normality and homoscedasticity, nonparametric tests were applied. Specifically, the Kruskal–Wallis test (α = 0,05). was used to assess significant differences among groups, and p-values were reported for each comparison. When appropriate, descriptive statistics were computed, including the mean, median, standard deviation, minimum and maximum values, and detection frequency for each individual PAH.

Multivariate analyses were performed to explore compositional patterns and potential PAH sources. A principal component analysis (PCA) with varimax rotation was applied after verifying sampling adequacy using the Kaiser–Meyer–Olkin measure (KMO ≥0.60) and Bartlett's test of sphericity ($p < 0.05$). The number of retained components was determined using Horn's parallel analysis (95th percentile). The resulting principal components were subsequently used as predictors in a multiple linear regression (MLR) model, with total PAH concentration as the dependent variable, to quantify source contributions.

Ecological risk was assessed using the mean effects range–median quotient (M-ERM-Q) method, whereas carcinogenic potential was estimated using the toxic equivalency factor approach (TEQ_carc). Spatial interpolation of risk indices was performed using kriging after fitting experimental semivariograms, and model performance was validated through cross-validation (bias close to zero, minimal RMSE, and a ratio of PLS error to variance close to 1).

All statistical analyses were carried out in Google Colaboratory using Python libraries (NumPy, Pandas, Seaborn, and Matplotlib) for data processing and visualization, and in ArcGIS Pro v3.1.0/ArcMap 10.8 for geospatial analyses.

3. Results

3.1. Identifications and quantifications PAHs

Total PAHs concentrations per sampling point ranged from 22.02 to 130.55 ng g^{-1}, with a mean of 55.26 ng g^{-1}. In the study area, LMW PAHs exhibited a higher mean concentration (37.38 ng g^{-1}) than HMW PAHs (17.88 ng g^{-1}).Two low molecular weight compounds, Nap and Flu, were detected in all samples. Among the quantified PAHs, Phe and Nap exhibited the highest mean concentrations (14.12 ng g^{-1} and 18.82 ng g^{-1}, respectively), followed by Flu (3.34 ng g^{-1}) and Dah (7.15 ng g^{-1}). Flt displayed the highest individual concentration, reaching 77.61 ng g^{-1}. In contrast, the high-molecular-weight compounds Bgp and Bkf showed mean concentrations below 1 ng g^{-1}, and their occurrence was inconsistent across samples (Table 3).

3.1.1. Comparison by altitudinal zone

The low-altitude zone exhibited the highest cumulative PAHs concentration (2516.6 ng g^{-1}), substantially exceeding those measured in the mid-altitude (1670.6 ng g^{-1}) and high-altitude zones (1172.8 ng g^{-1}) (Fig. 2a), showing a number of heterogeneous samples by altitude zone, with no significant differences in concentrations ($p > 0,05$) (Table 4). Moreover, the low-altitude zone displayed a noticeably broader interquartile range (24.8) compared with the mid-altitude (23.65) and high-altitude zones (23.67) (Fig. 2b), indicating greater spatial heterogeneity in PAHs concentrations at lower elevations.

Low molecular weight PAHs (2-3 rings) dominated the total PAHs load across all altitudinal zones, accounting for 67.9% of the total concentration in the high zone, 64.4% in the mid-zone, and 69.6% in the low-zone. Among the high molecular weight PAHs (4-6 rings), four-ring compounds contributed the most (low zone: 21.8%, mid zone: 25.1%, high zone: 24.7%), followed by five-ring PAHs (high zone: 3.9%, mid zone: 8.8%, low zone: 8.2%), while six-ring PAHs represented the smallest proportions (low zone: 0.4%, mid zone: 1.7%, high zone: 3.4%) (Fig. 3).

The average concentrations of Nap, Phe, and Flt showed clear dominance across all altitudinal zones. Nap exhibited the highest mean concentration in the low zone (20.66 ng g^{-1}), followed by the mid (18.09 ng g^{-1}) and high zones (16.23 ng g^{-1}). Flu displayed a similar trend, with greater concentrations at lower altitudes (low zone: 3.51 ng g^{-1}). Phe also recorded elevated levels in the low zone (14.78 ng g^{-1}). In contrast, Flt reached its maximum concentration in the mid zone (8.30 ng g^{-1}), followed by the low zone (7.63 ng g^{-1}). Acy and BaP were detected at consistently low concentrations (<1 ng g^{-1}) across all zones. DahA exhibited higher concentrations in the low (3.45 ng g^{-1}) and mid zones (3.37 ng g^{-1}), whereas IcdP was more abundant in the high zone (1.50 ng g^{-1}) (Fig. 4).

Soil pH, organic matter, and texture (% sand, % silt, and % clay) showed no significant differences among altitudinal zones. In contrast, available phosphorus varied significantly, with higher concentrations in the low zone ($p = 0.02$). Consistently, electrical conductivity was also significantly higher in the low zone ($p = 0.002$) (Fig. S1). In the correlation analysis, the variables most strongly associated with ΣPAHs were organic carbon ($\rho = 0.45$), organic matter ($\rho = 0.44$), sand fraction ($\rho = -0.42$), and silt fraction ($\rho = 0.40$). A similar pattern was observed for ΣLMW-PAHs, with stronger correlations with sand ($\rho = -0.55$) and silt ($\rho = 0.41$), followed by organic carbon ($\rho = 0.38$), clay ($\rho = 0.38$), and organic matter ($\rho = 0.37$). By contrast, ΣHMW-PAHs showed weak associations with the evaluated soil properties ($|\rho| < 0.24$) (Fig. 5).

3.1.2. Comparison by phenological stage and agronomic management practices

The seedling stage exhibited the highest mean PAHs concentration (60.4 ng g^{-1}), followed by the ripening (55.7 ng g^{-1}), filling (49.0 ng g^{-1}), and tillering (47.2 ng g^{-1}) stages. Among agronomic management practices, the burning treatment showed the highest average concentration (77.7 ng g^{-1}), followed by the resting condition (50.0 ng g^{-1}) (Fig. 6a). Regarding data dispersion, the burning practice displayed the widest interquartile range (46.17), followed by the seedling (29.39), ripening (28.33), filling (27.48), resting (23.27), and tillering (18.41) stages (Fig. 6b). A heterogeneous number of samples was recorded across phenological phases and agronomic practices; however, no significant differences in concentrations were observed ($p > 0.05$)

Table 3
Descriptive statistics of PAHs concentrations in soil samples (ng g^{-1}).

HAP	Mean	Median	Std	Range	Frequency	Detection (%)
Nap	*18.82*	*17.70*	*6.18*	*6.26–43.68*	*97*	*100*
Ace	*0.27*	*0.00*	*1.78*	*0.00–16.81*	*4*	*4*
Flu	*3.34*	*3.26*	*0.99*	*1.48–7.39*	*97*	*100*
Phe	*14.12*	*13.62*	*5.37*	*0.00–24.00*	*96*	*99*
Ant	*0.84*	*0.85*	*0.34*	*0.00–1.82*	*94*	*97*
Flt	*7.43*	*0.00*	*15.62*	*0.00–77.61*	*24*	*25*
Pyr	*3.38*	*3.37*	*1.64*	*0.00–8.77*	*91*	*94*
BaA	*0.17*	*0.00*	*0.46*	*0.00–2.22*	*17*	*18*
Chr	*1.98*	*1.98*	*2.08*	*0.00–10.28*	*57*	*59*
Bbf	*0.96*	*0.89*	*1.01*	*0.00–5.90*	*66*	*68*
Bkf	*0.36*	*0.33*	*0.34*	*0.00–1.94*	*75*	*77*
BaP	*0.12*	*0.00*	*0.46*	*0.00–2.22*	*6*	*6*
Dah	*2.67*	*0.00*	*6.58*	*0.00–24.93*	*36*	*37*
Bgp	*0.15*	*0.00*	*0.36*	*0.00–1.67*	*20*	*21*
Ind	*0.67*	*0.00*	*2.05*	*0.00–10.24*	*11*	*11*
ΣPAHs	*55.26*	*52.07*	*23.67*	*22.02–130.55*	*97*	*100*
ΣLMW_PAHs	*37.38*	*35.18*	*11.40*	*16.69–75.56*	*97*	*100*
ΣHMW_PAHs	*17.88*	*9.25*	*19.35*	*0.67–83.59*	*97*	*100*

Note. *The values were calculated using all samples (n = 97), including non-detects recorded as 0. ΣPAHs corresponds to the sum of the 15 quantified PAHs. ΣLMW PAHs corresponds to the sum of Nap, Ace, Flu, Phe, and Ant; ΣHMW PAHs corresponds to the sum of Flt, Pyr, BaA, Chr, Bbf, Bkf, BaP, Dah, Bgp, and Ind.*

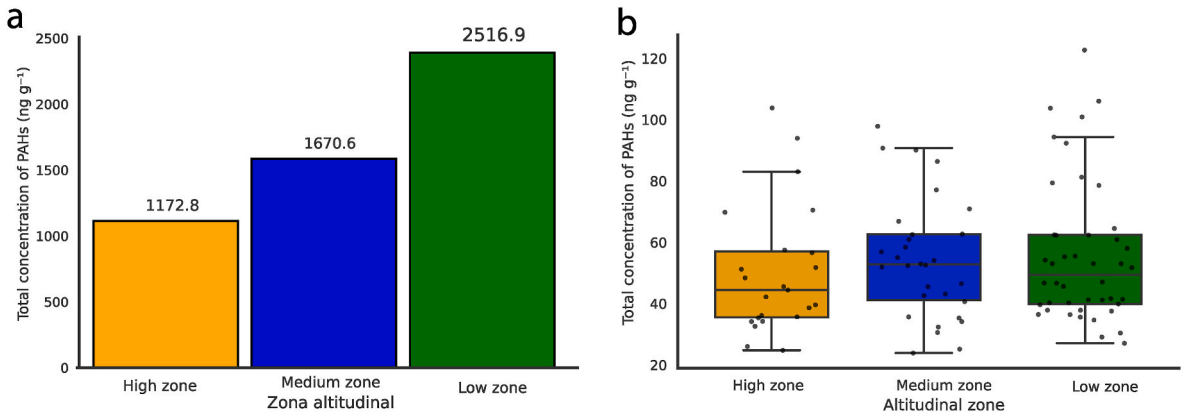

Fig. 2. Distribution of total PAHs concentrations across altitudinal zones: (a) cumulative PAHs load (ng m^{-2}) and (b) boxplot of total PAHs concentrations (ng m^{-2}) by altitude zone. Altitudinal zones are defined as low (383-488 m a.s.l.), medium (488-640 m a.s.l.), and high (640-1052 m a.s.l.).

Table 4
Descriptive statistics of PAHs concentrations in soil samples (ng g^{-1}).

Zone	Number of samples	Kruskal-Wallis (p-value)
Hight	*23*	*0.4259*
Middle	*30*	
Low	*44*	

(Table 5). The distribution of individual PAHs concentrations by compound is presented in Fig. S2.

The ripening and resting phases exhibited the greatest chemical diversity, with 15 PAHs compounds detected. The seedling phase followed, with 14 PAHs identified, while Acy was not detected (Fig. 7). In the tillering and filling phases, 13 compounds were identified, with the absence of BaA and IcdP in the former, and Acy and BghiP in the latter. Conversely, the burning practice showed the lowest chemical diversity (nine PAHs), due to the absence of Acy, BaA, BaP, BghiP, DahA and IcdP. Despite this, the burning condition exhibited elevated mean concentrations of Flt (27.54 ng g^{-1}), Nap (20.43 ng g^{-1}), and Phe (19.15 ng g^{-1}).

The multivariate variation in PAHs concentrations as a function of rice phenological stages and agronomic management practices is illustrated in Fig. 8. The first two principal components (PC1 and PC2) jointly explained 42.7% of the total variance (PC1 = 23.8%, PC2 = 18.9%). The seedling stage exhibited a compact and centralized distribution, indicating lower variability in PAHs composition. In contrast, the tillering and ripening stages showed greater dispersion, reflecting higher heterogeneity in PAHs concentrations. The resting stage was slightly separated along positive PC1 values, whereas the filling and burning stages overlapped with other groups, preventing clear differentiation among them.

3.2. Sources of PAHs

The cross-diagnostic ratio Flt/(Flt + Pyr) indicated a predominance of pyrogenic sources (values > 0.50), mainly associated with the combustion of coal, wood, and grass, with a smaller subset of samples suggesting petrogenic contributions (Fig. 9). Among the pyrogenic sources, the IcdP/(IcdP + BghiP) ratio revealed the coexistence of emissions from fossil fuel combustion and coal/wood/grass burning, with the former being slightly more dominant (Fig. 9a). The Flt/(Flt + Pyr) cross-plot exhibited greater data dispersion within the pyrogenic domain (values > 0.50), whereas the remaining samples clustered near 0, consistent with petrogenic contributions. Conversely, the Ant/(Ant + Phe) ratio (<0.10) suggested a predominance of petroleum derived sources, accompanied by a relative decline in combustion-related signatures (Fig. 9b).

In the rotated principal component analysis (PCA), the first three principal components (PCs) were retained according to Horn's parallel

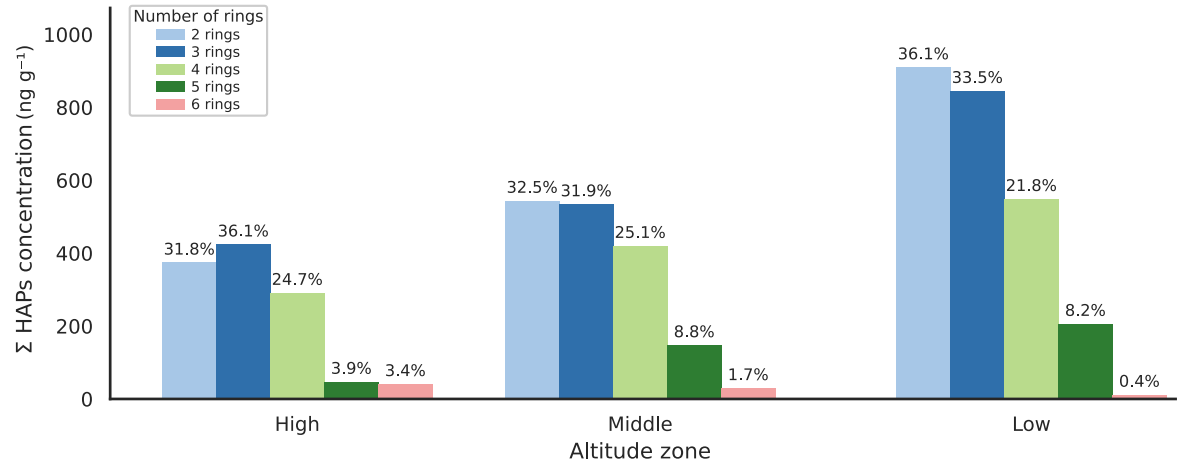

Fig. 3. Percentage distribution of PAHs classified by the number of aromatic rings across altitudinal zones. Altitudinal zones are defined as follows: low (383-488 m a.s.l.), medium (488-640 m a.s.l.), and high (640-1052 m a.s.l.). Colors indicate the following: light blue = 2 rings, blue = 3 rings, light green = 4 rings, dark green = 5 rings, and pink = 6 rings.

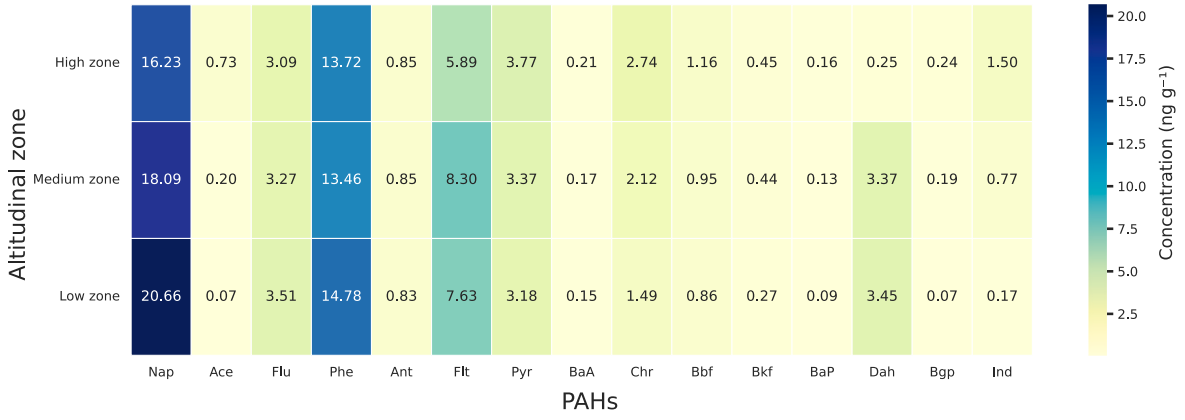

Fig. 4. Concentrations of PAHs in rice agricultural soils across altitudinal zones. Each cell represents the mean concentration of individual PAHs (ng g^{-1}). Color intensity indicates concentration magnitude, with darker tones representing higher levels. Altitudinal zones are defined as low (383-488 m a.s.l.), medium (488-640 m a.s.l.), and high (640-1052 m a.s.l.).

analysis (eigenvalue = 1.53). Together these components explained 53% of the total variance, with PC1 accounting for 22%, PC2 for 20%, and PC3 for 11% (Table S3). The Varimax-rotated loading profiles RC1 exhibited high loadings Phe (0.91), Ant (0.82), Pyr, (0.79), Nap (0.74), and Flu (0.62) (Fig. 10a). In contrast, RC2 showed strong loadings for high-molecular-weight PAHs such as BkF (0.86), BbF (0.75), BaA (0.72), and BaP (0.68) (Fig. 10b). RC3 was mainly associated with DahA, (0.66), Flt (0.57), Flu (0.54), IcdP (0.45), and BghiP (0.45) (Fig. 10c). The multiple linear regression (MLR) analysis revealed that the relative source contributions to ΣPAHs, quantified as fractional percentages of the total absolute standardized effect (|β*|), were 42.1% for RC1 ($p < 0.05$), 5.4% for RC2 ($p > 0.05$) and 52.3% for RC3 ($p < 0.05$) (Tables S4 and S5). The overall model (Equation (7)) achieved a coefficient of determination (R^2) of 0.71.

$$\sum HAPs = 6.483\ RC1 - 0.865\ RC2 + 11.364\ RC3 + 55.259 \quad \text{(Equation 7)}$$

3.3. Assessment of ecological risks and carcinogenic factors

As shown in Fig. 11a, the ecological risk map indicates that the assessed area did not exceed the critical effect concentration (CEC = 290 ng g^{-1}). However, classification into three concentration ranges low (4.02 - 4.76 μg g^{-1}), medium (4.76 - 5.25 μg g^{-1}), and high (5.25-6.02 μg g^{-1}) revealed elevated PAHs concentrations in the southwest (near the city of Jaén), northwest (downstream of the Jaén wastewater treatment plant), and southeast (at the mouth of the Amójú River and to the Bellavista treatment plant). The least contaminated zones were located in the northwest (areas irrigated by the Tumbillán stream), north (upland areas near Santa Cruz).The high-contamination zone covered approximately 1142.022 ha, the moderate contamination zone encompassed 3702.68 ha, and the low-contamination zone extended over 833.43 ha (Fig. 11a). The agricultural region of Jaén Province was classified as low ecological risk (M-ERM-Q = 0.0112), with values ranging from 0.00116 to 0.00856 (Fig. 11b). The highest contamination levels were observed in the northwest of Shanango, the northeast of Bellavista, and areas adjacent to Santa Cruz. Regarding carcinogenic risk, the TEQ_{CARC} indicated that medium high risk areas accounted for 62% of the total, followed by low risk (37.24%), high risk (0.16%), and no-risk (0.007%) zones (Fig. 11c). The cumulative concentration for all analyzed samples was 282.84 ng BaP_{eq} g^{-1}, and the areas with the highest TEQ_{CARC} values spatially coincided with the high-risk zones identified by the M-ERM-Q index.

4. Discusión

This study assessed the concentrations of 15 PAHs in rice-growing areas within the Amojú River basin. The mean concentration was

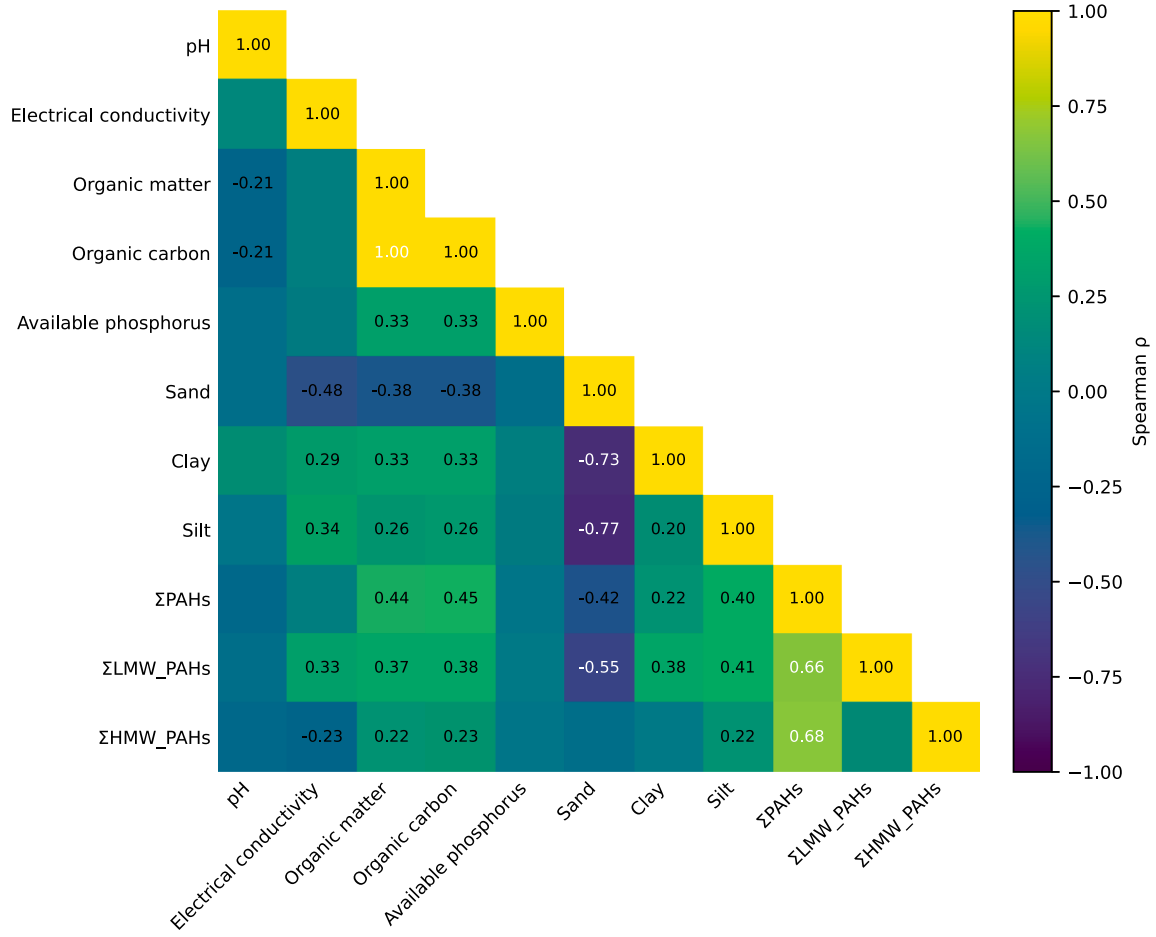

Fig. 5. Spearman correlation matrix between soil physicochemical properties and PAH indicators. The heatmap shows pairwise Spearman's rho (ρ) values among pH, electrical conductivity, organic matter, organic carbon, available phosphorus, soil texture fractions (sand, clay, silt), and PAH metrics (ΣPAHs, ΣLMW_PAHs, ΣHMW_PAHs).

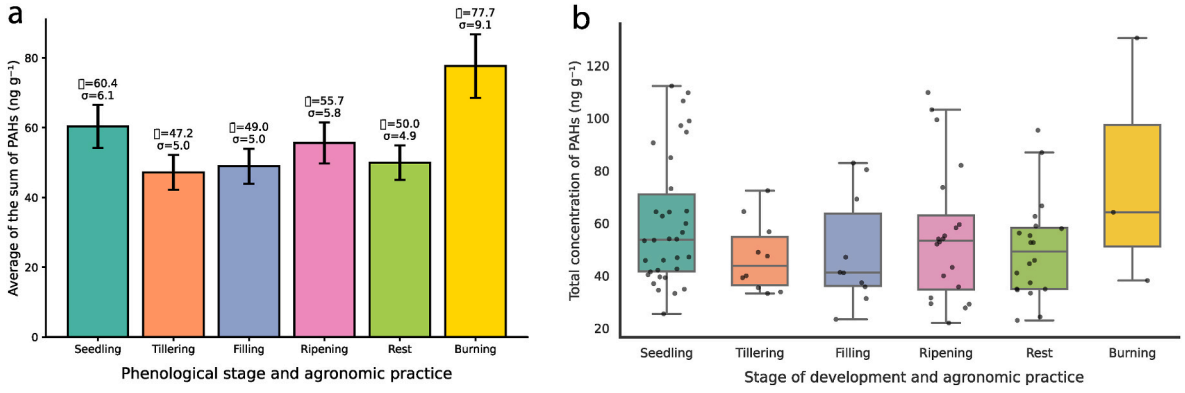

Fig. 6. Concentrations of PAHs according to phenological stages and agronomic management practices: (a) mean PAHs concentrations by phenological stage and management practice, and (b) data distribution.

55.26 ng g^{-1}, which is lower than those reported for other major rice producing regions in Asia. For example, average concentrations of 118 ng g^{-1} have been reported in the Hani Terrace, 171 ng g^{-1} in the Sanjiang Plain, 329 ng g^{-1} in the Taihu Plain, and 352.94 ng g^{-1} in Suzhou [14]. These differences may be attributed to the higher population densities in those regions [32,61] and their proximity to industrial zones [32], factors known to increase pollutant accumulation [14]; another important factor is the sampling depth, which in this study was relatively greater (0–30 cm). In other crops, a tendency for PAH concentrations to decrease with depth has been reported [39]; therefore, this wider sampling interval could contribute to lower measured concentrations and limit comparability with studies that use shallower depths. However, the specific influence of depth on PAH concentrations in paddy soils is not yet clearly established. In this regard, future research should explicitly assess the effect of sampling depth under flooded conditions, with particular emphasis on the rhizosphere, where

Table 5
Number of samples for Phenological phases and agronomic practices.

Phenological phases and agronomic practices	Number of samples	Kruskal-Wallis (p-value)
Seedling	*34*	*0.4406*
Tillering	*10*	
Filling	*10*	
Ripening	*20*	
Burning	*3*	
Rest	*20*	

the combined action of microbial communities which tend to degrade PAHs [21] and plant roots which can absorb low molecular weight PAHs and adsorb high molecular weight PAHs [16,19,20]. may reduce bioavailability and, consequently, the dermal-contact toxicity potential [41].

The persistence of Nap and Flu observed in this study may be explained by their high emission rates and elevated volatility and solubility, which facilitate both atmospheric and fluvial transport [14]. In addition, soil organic carbon was positively associated with PAHs, showing direct correlations with ΣPAHs ($\rho = 0.45$) and ΣLMW-PAHs ($\rho = 0.38$). Notably, the strongest relationship was the negative correlation between ΣLMW-PAHs and sand content ($\rho = -0.55$), suggesting that sandier soils with lower sorption capacity promote greater mobility of LMW compounds, particularly under flooded conditions [62]. Overall, although PAHs concentrations in the Amojú basin were lower than those reported for Asian rice growing regions, the predominance of low molecular weight PAHs suggests the influence of local emission sources, which should be considered in the formulation of management and mitigation strategies.

Overall, the distribution of PAHs was widespread, with no statistically significant differences among altitudinal zones ($p > 0,05$), as differences are easier to detect when between-group variability is large and within-group variability is small [63]. However, descriptive statistics indicated higher concentrations recorded at lower elevations (Fig. 2a), which may be attributed to the topographic characteristics of the Amojú River basin, where runoff promotes the accumulation of pollutants in low-lying areas [14,64,65]. Due to their hydrophobic nature, these compounds are prone to transport via water flow toward flatter terrain [14,65]. In contrast, high molecular weight PAHs exhibited greater variability with altitude (Fig. 3), likely due to their higher molecular mass and stronger affinity for adsorption onto the solid phase of soils [66]. This behavior suggests the coexistence of two primary accumulation mechanisms: mobility and deposition in low-lying zones for low molecular weight PAHs, and edaphic retention for high molecular weight compounds.

Regarding phenological stages, the highest concentrations of PAHs were recorded during the seedling stage (Fig. 5), likely due to the incorporation of ash from stubble burning and the input of low molecular weight PAHs transported through irrigation water [14,65,67]. It is important to note that these variations reflect descriptive trends rather than statistically significant differences. During the tillering, filling, and ripening stages, PAHs concentrations tended to decrease [68], which may be attributed to the activity of soil bacterial communities that enhance PAHs degradation throughout the crop cycle [68]. With respect to agronomic management practices, the resting stage exhibited the lowest PAHs concentrations (Fig. 5), possibly due to continuous microbial degradation [69], reduced contaminant input via irrigation, and improved soil oxygenation following drying, which promotes aerobic degradation of PAHs [21]. Conversely, the burning practice showed the highest PAHs concentrations, likely due to the pyrolysis of organic matter, consistent with the elevated presence of fluoranthene (Flt) (Fig. 6), a compound typically associated with combustion processes [14,70]. These differences should be interpreted as observational patterns, as no statistically significant differences were detected among management practices. These findings indicate that both phenological stages and, in particular, agronomic management practices influence the dynamics of PAHs in rice cultivation systems. Although variations in PAHs concentrations and trends were observed, no statistically significant differences were detected among phenological stages or management practices ($p > 0,05$), as evidenced by the limited separation in the principal component analysis (Fig. 7). Although linear mixed models (LMMs) and generalized linear mixed models (GLMMs) can accommodate combinations of factors [71], unbalanced designs tend to introduce identifiability issues and unstable parameter estimates, which can weaken standard inference [72]. Therefore, future studies should adopt a balanced sampling design with a homogeneous number of samples per stage and management practice, or implement temporal monitoring, to enable more robust inferences regarding differentiation patterns.

Regarding the origin of PAHs, the diagnostic ratios indicated the coexistence of sources associated with biomass and fossil fuel combustion (Fig. 8a), with a slight bias toward petroleum-related inputs (Fig. 8b). According to the principal component analysis-multilinear regression (PCA-MLR) results, PC3 the primary source of PAHs, explaining 52.3% of the total variance showed elevated loadings for DahA, Flt, Flu, BghiP, and IcdP, compounds commonly associated with gasoline and diesel vehicle emissions [23,73–76]. This suggests a continuous influence of vehicular activity in areas to rice cultivation. Conversely, PC1 (42.1% of explained variance) exhibited high loadings for Phe, Pyr, and Flu, characteristic of biomass combustion [26,74], along with Nap and Ant, which are typically found in unburned petroleum sources [22,23]. These results indicate the combined presence of

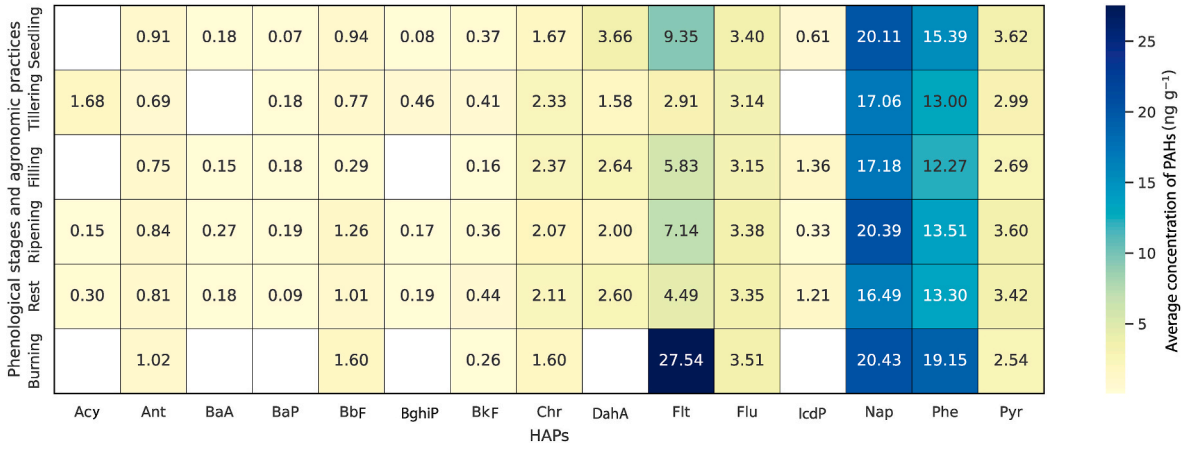

Fig. 7. Distribution of PAHs as a function of rice phenological stages and agronomic management practices. Each cell represents the mean PAHs concentration (ng g^{-1}). Color intensity indicates concentration magnitude, with darker tones representing higher levels. White cells denote compounds that were not detected.

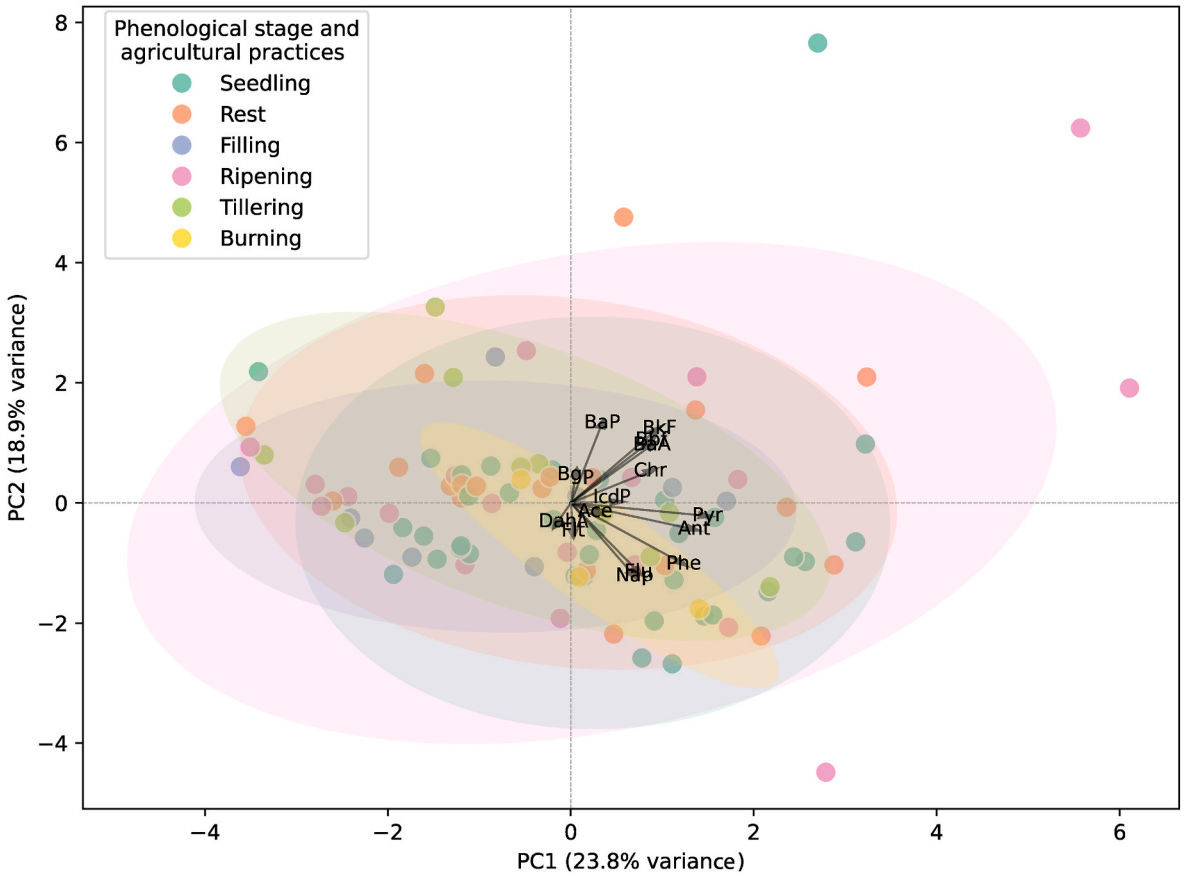

Fig. 8. Principal component analysis (PCA) of PAHs concentrations in relation to phenological stages and agronomic management practices in rice cultivation. The biplot illustrates sample distributions along the first two principal components (PC1 and PC2), with 95% confidence ellipses for each stage and loading vectors representing PAHs variables.

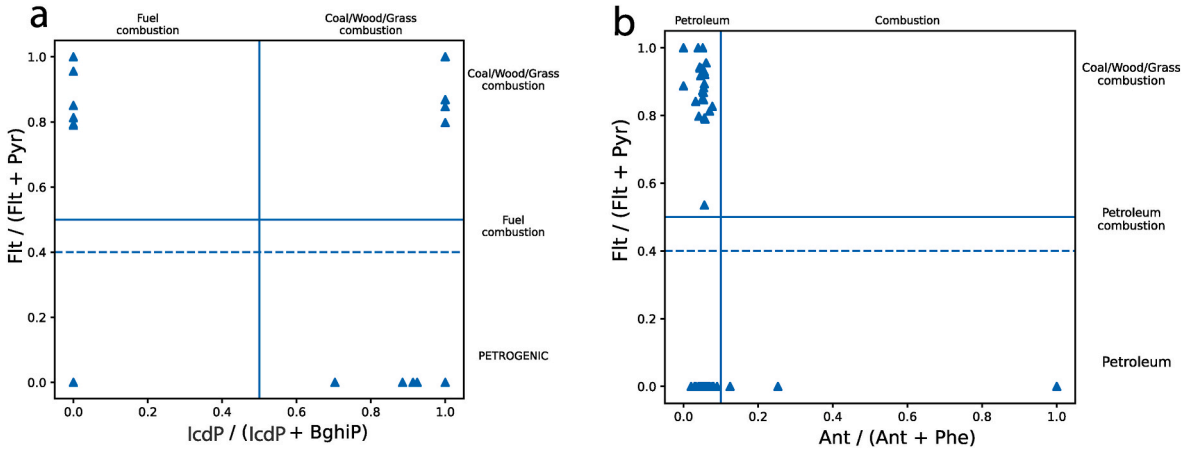

Fig. 9. Cross plots of diagnostic ratios for the identification of PAHs sources. (a) Relationship between Flt/(Flt + Pyr) and Ind/(Ind + BghiP). (b) Relationship between Flt/(Flt + Pyr) and Ant/(Ant + Phe).

pyrogenic and petrogenic PAHs, likely introduced through contaminated irrigation water [39,65]. PC2, which accounted for 5.4% of the explained variance, showed high loadings for BkF, BbF, and BaP markers of vehicular emissions [23,75] as well as BaA and Chr, typical indicators of coal combustion [74]. The relatively low contribution of this component may reflect the limited use of coal in the city of Jaén compared with other urban areas where coal is used for heating during winter [73].

The analysis identified PAHs sources with reasonable accuracy (R^2 = 0.71). However, the cumulative variance explained by the first three principal components (53%) was insufficient for definitive source characterization when compared with previous studies [26,73,77]. This limitation is likely related to the complex environmental behavior of PAHs, whose persistence in soil is governed by degradation dynamics influenced by soil texture, organic carbon content, nutrient availability, moisture, and aeration [78]. Consequently, future studies should incorporate assessments of the topsoil layer (0-10 cm) across a wider range of sampling sites within the Amojú River basin and other rice

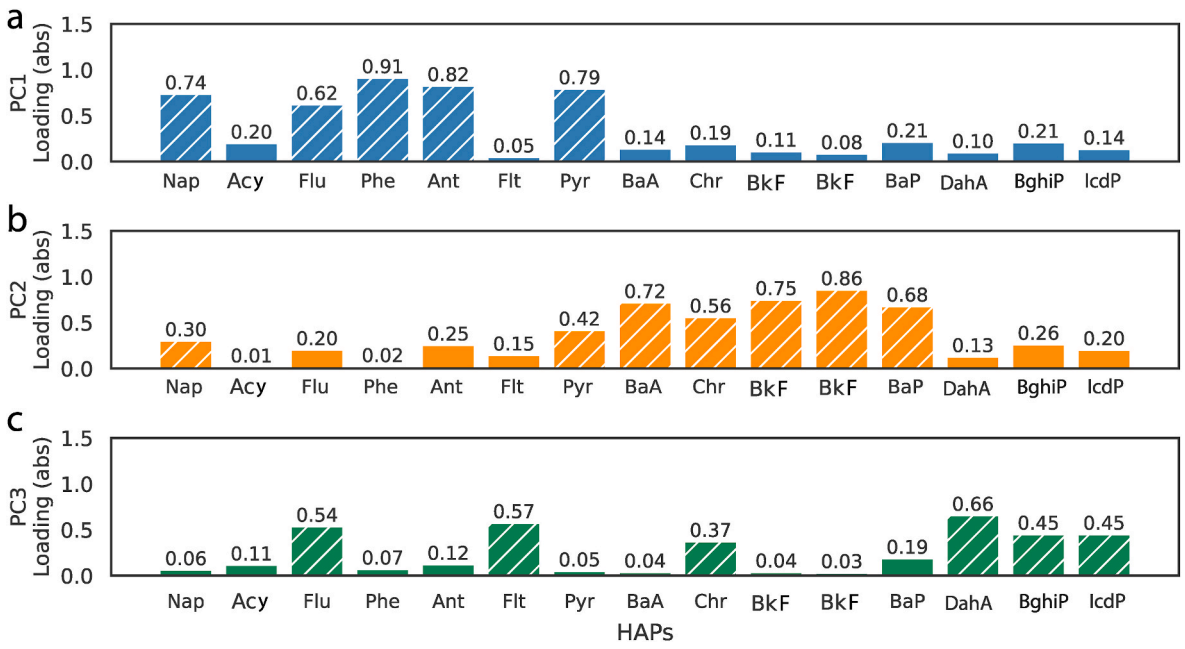

Fig. 10. Absolute loadings of PAHs on the first three principal components (a-b: PC1-PC3) derived from principal component analysis (PCA). Striped bars indicate loading values greater than 0.30.

producing regions to more accurately elucidate the origin, transport, and environmental fate of PAHs in agricultural soils.

Regarding ecological risks, the carbon normalization method indicated that PAHs concentrations remained below the reference threshold of 290 μg g^{-1} (Fig. 10a). However, higher PAHs concentrations were observed in areas located near human settlements and wastewater treatment plants. Therefore, future research should prioritize identifying potential pollution sources in zones to urban areas and establish monitoring programs to evaluate the quality of irrigation water. According M-ERM-Q approach, the study area was classified as low risk (<0.1), although certain localized zones exhibited elevated contamination levels (Fig. 10b). These zones were primarily characterized by high concentrations of DahA, a compound typically associated with fossil fuel combustion [23,75]. Furthermore, the interpolated total equivalent carcinogenic concentration (TEQ_{CARC}) values indicated low carcinogenic potential, ranging from 0.0083 to 18.7483 ng BaP_{eq} g^{-1}. These levels are substantially lower than those reported for rice growing regions in China and Nigeria (251.96-2348 ng BaP_{eq} g^{-1}) and remain well below the Canadian Soil Quality Guideline threshold of 600 ng BaP_{eq} g^{-1} [41]. M-ERM-Q and TEQCARC correspond to a relative classification based on numerical ranges and are used mainly to identify spatial heterogeneity and delineate priority areas within the site, whereas (ii) comparison with guideline/threshold values (e.g., <600 ng BaP_eq g^{-1}) constitutes a distinct criterion aimed at assessing potential exceedances relative to reference values. Implications for human health are inferred solely from the soil TEQ, given that PAHs were not measured in rice grains, irrigation water, or air; therefore, future studies are recommended to evaluate exposure matrices and pathways.

Research on the presence, distribution, and risks associated with PAHs in soils is essential for the environmental characterization of agricultural landscapes. Such investigations enable the identification of contamination hotspots, the inference of emission sources, and the assessment of ecological and human health risks. These insights provide a solid foundation for developing mitigation strategies to reduce pollutant loads in rice growing soils. This study represents the first systematic evaluation of PAHs in rice cultivation areas in Peru, focusing on the lower Amojú River basin, where we identified urban areas and sites downstream of wastewater treatment plants as critical hotspots of PAH accumulation; through irrigation, these contaminants can be transported and retained in rice fields. At the national level, Peru has regulatory instruments to support environmental monitoring and compliance, including Environmental Quality Standards (ECAs) for water bodies [79] y and Maximum Permissible Limits (LMPs) for effluents from Domestic or Municipal Wastewater Treatment Plants (WWTPs) [80]; In addition, regulations addressing agricultural and agro-industrial residue management prohibit the open burning of agricultural residues, providing a framework to reduce emissions and protect air, water, and soil quality [81]. Together, these instruments strengthen the oversight of water and soil resources and are further supported by the implementation of regulations that govern water user organizations, reinforcing their participation in multisectoral water resources management [82]. These regulatory frameworks support efforts to improve the environmental quality of the agricultural region, and this study draws attention to agricultural soil contamination while also proposing a methodological approach for environmental monitoring in these rice-growing areas that sustain the livelihoods of thousands of local farmers. Nevertheless, important knowledge gaps remain, particularly regarding the seasonal and interannual variability of PAHs concentrations and their translocation within rice plants. Future research should incorporate additional environmental matrices, including water and sediments, to achieve a comprehensive understanding of the potential risks that PAHs pose to human health, crop sustainability, and soil resource conservation.

5. Conclusions

This study evaluated the concentrations of 15 PAHs in soils from the Amojú River basin, revealing no statistically significant differences (p > 0,05) across altitudinal zones or agronomic management practices. Nevertheless, a clear trend of increasing PAHs concentrations with decreasing altitude was observed. Across phenological stages and management practices, elevated PAHs levels were particularly associated with stubble burning. Source apportionment analysis indicated that vehicular emissions were the dominant contributors (52.3%), followed by biomass combustion and petroleum-derived sources (42.1%), whereas coal combustion accounted for the smallest fraction (5.4%). In terms of ecological risk, both the carbon normalization and M-ERM-Q methods classified the area as low risk, with values ranging from 4.02 to

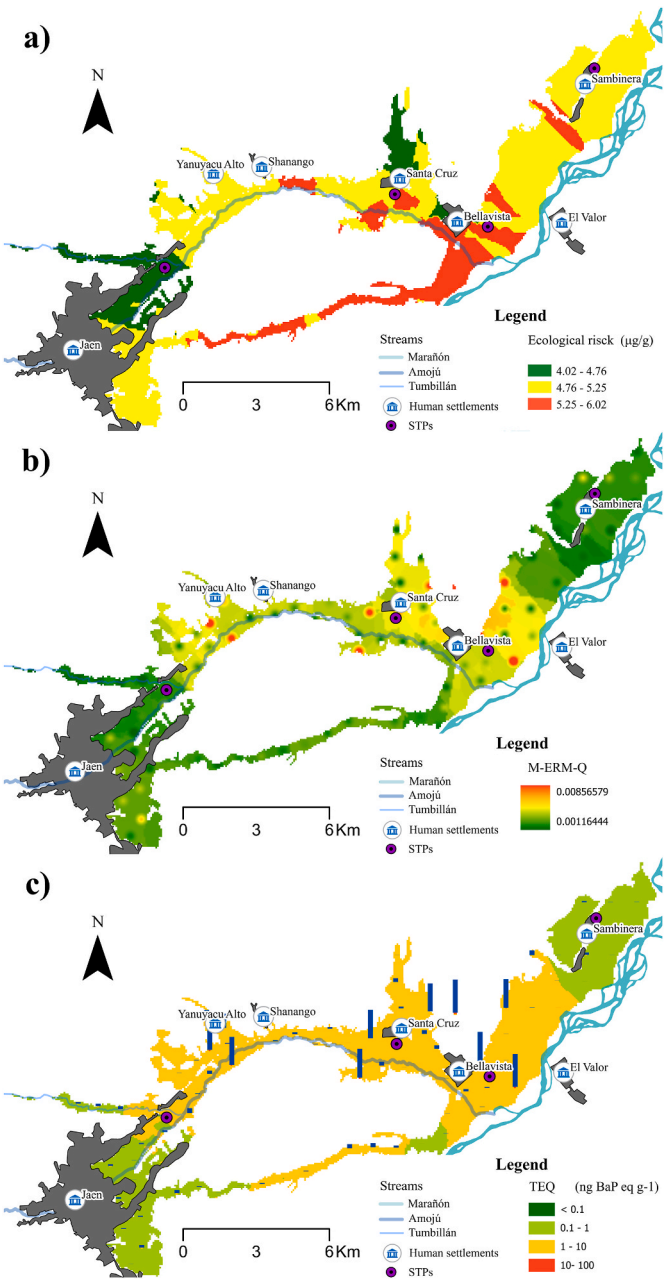

Fig. 11. Ecological risk and carcinogenic potential maps for PAHs: (a) ecological risk map based on the carbon normalization method; (b) ecological risk map derived from M-ERM-Q method; and (c) potential carcinogenic risk map based on the TEQ_{CARC} method.

6.02 and 0.00116 to 0.00856, respectivel. However, localized hotspots were identified near human settlements, wastewater treatment plants, and the mouth of the Amojú River. Carcinogenic risk assessment showed that the highest TEQ_{CARC} values (0.0083 to 18.7483 ng BaP_{eq} g^{-1}) were confined to small areas and remained below both the Peruvian Soil Quality Standard (ECA) and the Canadian Soil Quality Guideline. DahA was identified as the primary contributor to overall carcinogenic potential. This research represents the first comprehensive assessment of PAHs contamination in rice-growing soils in Peru, underscoring the influence of altitude and agronomic practices on their distribution. While the results suggest a generally low ecological and carcinogenic risk under current soil quality standards, further investigation is warranted to evaluate potential pathways of human exposure, particularly through PAH transfer to rice grains and dietary intake. The findings highlight the need for continued monitoring to identify pollution sources, assess impacts on agricultural productivity, and evaluate potential risks to human health.

CRediT authorship contribution statement

Cristian Culqui: Writing – original draft, Validation, Software, Methodology, Investigation, Formal analysis, Data curation. **Daniel Tineo:** Writing – review & editing, Visualization, Supervision, Software, Project administration, Investigation, Formal analysis, Conceptualization. **Jorge A. Fernández-Jibaja:** Visualization, Validation, Software, Methodology, Investigation, Formal analysis, Data curation. **Yeltsin A. Álvarez-Robledo:** Writing – original draft, Validation, Methodology, Investigation, Data curation, Conceptualization. **Larry D. Garcia-Frias:** Writing – original draft, Validation, Software, Methodology, Investigation, Formal analysis, Data curation. **Jani Mendoza-Merino:** Visualization, Validation, Methodology, Investigation, Conceptualization. **Victor H. Taboada-Mitma:** Validation, Supervision, Resources, Project administration, Investigation, Funding acquisition. **Juancarlos Cruz-Luis:** Visualization, Validation, Supervision, Resources, Project administration, Investigation, Funding acquisition. **Nilton B. Rojas-Briceño:** Writing – review & editing, Visualization, Validation, Methodology, Investigation, Conceptualization. **Ligia García:** Visualization, Validation, Methodology, Investigation, Conceptualization. **Franz Zirena Vilca:** Writing – review & editing, Visualization, Validation, Investigation, Formal analysis. **Malluri Goñas:** Writing – review & editing, Visualization, Validation, Supervision, Software, Methodology, Investigation, Conceptualization.

The ethical declaration

We declare that this article is entirely original and constitutes an intellectual contribution by the authors participating in this study.

Availability of data

The datasets generated and analyzed in this study are available from the authors upon request.

Declaration of competing interest

The authors declare that they have no known competing financial interests or personal relationships that could have appeared to influence the work reported in this paper.

Appendix A. Supplementary data

Supplementary data to this article can be found online at https://doi.org/10.1016/j.jafr.2026.102726.

Data availability

Data will be made available on request.

References

[1] W. Agustiono, K.E. Permana, C. Chan, D.A. Dewi, M.M.R. Al Husain, Rice Variety Identification Based on Transfer Learning Architecture Using DENS-INCEP, IEEE, 2025, pp. 78007–78020, https://doi.org/10.1109/ACCESS.2025.3562585. Access 13.

[2] A.A. Chandio, D. Ozdemir, Y. Jiang, Modelling the impact of climate change and advanced agricultural technologies on grain output: recent evidence from China, Ecol. Model. 485 (2023), https://doi.org/10.1016/J.ECOLMODEL.2023.110501.

[3] S.S. Mohapatra, T.B. Bagchi, A. Mahanty, T. Adak, M.K. Panda, K. Chattopadhyay, Development of prediction models for high throughput phenotyping of protein and essential amino acids content in rice grain using the near infrared reflectance spectroscopy, J. Food Compos. Anal. 142 (2025) 107453, https://doi.org/10.1016/J.JFCA.2025.107453.

[4] Food and Agriculture Organization [FAO], Panorama de la seguridad alimentaria y nutricional en América latina y el Caribe. http://190.96.97.141:8889/xmlui/handle/123456789/178, 2023.

[5] Food and Agriculture Organization [FAO], Cultivos Y Productos de Ganadería, FAOSTAT, 2025. https://www.fao.org/faostat/es/#data/QCL/visualize. (Accessed 14 January 2026).

[6] Ministerio de Agricultura y Riego [MIDAGRI], Perfil productivo y competitivo de los principales cultivos del sector. https://app.powerbi.com/view?r=eyJrIjoiYjYwYTk5MDgtM2M0MS00NDMyLTgzNDEtMjNhNjEzYWQyOTNlIiwidCI6IjdmMDg0NjI3LTdmNDAtNDg3OS04OTE3LTk0Yjg2ZmQzNWYzZiJ9, 2025.

[7] Ministerio de Agricultura y Riego [MIDAGRI], Perfil productivo y competitivo de los principales cultivos del sector. https://app.powerbi.com/view?r=eyJrIjoiYjYwYTk5MDgtM2M0MS00NDMyLTgzNDEtMjNhNjEzYWQyOTNlIiwidCI6IjdmMDg0NjI3LTdmNDAtNDg3OS04OTE3LTk0Yjg2ZmQzNWYzZiJ9, 2025. (Accessed 16 August 2025).

[8] M. van Dijk, T. Morley, M.L. Rau, Y. Saghai, A meta-analysis of projected global food demand and population at risk of hunger for the period 2010–2050, Nat. Food 2 (2021) 494–501, https://doi.org/10.1038/s43016-021-00322-9.

[9] A. Hamad, A. Tayel, Food 2050 concept: trends that shape the future of food, J. Future Foods (2025), https://doi.org/10.1016/J.JFUTFO.2025.03.003.

[10] United Nations [ONU], World population prospects - population division. https://population.un.org/wpp/, 2019.

[11] J. Parshad, R. Kumar, V. Chhokar, N. Patil, V. Beniwal, N. Singh, A. Kumar, N. Singh, R. Yogi, M. Kumar, P. Vikram, A. Chauhan, A. Kumar, Rice residue management: alternative strategies and emerging technologies for a sustainable ecosystem, Pedosphere 35 (2025) 53–66, https://doi.org/10.1016/J.PEDSPH.2024.06.004.

[12] G. Singh, N. Kaur, R. Khanna, R. Kaur, S. Gudi, R. Kaur, N. Sidhu, Y. Vikal, G. S. Mangat, 2Gs and plant architecture: breaking grain yield ceiling through breeding approaches for next wave of revolution in rice (Oryza sativa L.), Crit. Rev. Biotechnol. 44 (2024) 139–162, https://doi.org/10.1080/07388551.2022.2112648.

[13] J. Xu, H. Wang, L. Sheng, X. Liu, X. Zheng, Distribution characteristics and risk assessment of polycyclic aromatic hydrocarbons in the momoge wetland, China, Int. J. Environ. Res. Publ. Health 14 (2017) 85, https://doi.org/10.3390/IJERPH14010085, 14 (2017) 85.

[14] D. Liu, L. Niu, Z. Guo, S. Mao, S. Liu, D. Xu, C. Xu, X. Sun, H. Yu, W. Liu, Polycyclic aromatic hydrocarbons in paddy soils: distribution, source apportionment, and risk assessment in major rice-growing regions of China, Environ. Chem. Ecotoxicol. 7 (2025) 935–943, https://doi.org/10.1016/J.ENCECO.2025.04.013.

[15] B.S. Fakinle, E.L. Odekanle, C. Ike-Ojukwu, O.O. Sonibare, O.A. Falowo, F. W. Olubiyo, D.O. Oke, C.O. Aremu, Quantification and health impact assessment of polycyclic aromatic hydrocarbons (PAHs) emissions from crop residue combustion, Heliyon 8 (2022) e09113, https://doi.org/10.1016/J.HELIYON.2022.E09113.

[16] J. Nie, Q. ming Wang, L. jun Han, J. shan Li, Synergistic remediation strategies for soil contaminated with compound heavy metals and organic pollutants, J. Environ. Chem. Eng. 12 (2024) 113145, https://doi.org/10.1016/J.JECE.2024.113145.

[17] M. Zhao, B. Tang, L. Bin, P. Li, S. Huang, F. Fu, Occurrence, distribution and removal of polycyclic aromatic hydrocarbons in a typical process for textile wastewater treatment of the Pearl River Delta Region, South China, J. Environ. Chem. Eng. 10 (2022) 107149, https://doi.org/10.1016/J.JECE.2022.107149.

[18] A. Amadou, D. Praud, C. Marques, H. Noh, P. Frenoy, A. Vigneron, T. Coudon, F. Deygas, G. Severi, B. Fervers, F.R. Mancini, Dietary intake of polycyclic aromatic hydrocarbons (PAHs) and breast cancer risk: evidence from the French E3N-Generations prospective cohort, Environ. Int. 200 (2025) 109505, https://doi.org/10.1016/J.ENVINT.2025.109505.

[19] A.B. Patel, S. Shaikh, K.R. Jain, C. Desai, D. Madamwar, Polycyclic aromatic hydrocarbons: sources, toxicity, and remediation approaches, Front. Microbiol. 11 (2020) 562813, https://doi.org/10.3389/FMICB.2020.562813/XML.

[20] X. Shang, S. Wu, Y. Liu, K. Zhang, M. Guo, Y. Zhou, J. Zhu, X. Li, R. Miao, Rice husk and its derived biochar assist phytoremediation of heavy metals and PAHs co-contaminated soils but differently affect bacterial community, J. Hazard. Mater. 466 (2024) 133684, https://doi.org/10.1016/j.jhazmat.2024.133684.

[21] H. Bao, J. Wang, H. Zhang, J. Li, H. Li, F. Wu, Effects of biochar and organic substrates on biodegradation of polycyclic aromatic hydrocarbons and microbial community structure in PAHs-contaminated soils, J. Hazard. Mater. 385 (2020) 121595, https://doi.org/10.1016/J.JHAZMAT.2019.121595.

[22] R.K. Larsen, J.E. Baker, Source apportionment of polycyclic aromatic hydrocarbons in the urban atmosphere: a comparison of three methods, Environ. Sci. Technol. 37 (2003) 1873–1881, https://doi.org/10.1021/es02061840206184.

[23] A. Motelay-Massei, D. Ollivon, B. Garban, K. Tiphagne-Larcher, I. Zimmerlin, M. Chevreuil, PAHs in the bulk atmospheric deposition of the seine river basin: source identification and apportionment by ratios, multivariate statistical techniques and scanning electron microscopy, Chemosphere 67 (2007) 312–321, https://doi.org/10.1016/J.CHEMOSPHERE.2006.09.074.

[24] C.R. Marris, S.N. Kompella, M.R. Miller, J.P. Incardona, F. Brette, J.C. Hancox, E. Sørhus, H.A. Shiels, Polyaromatic hydrocarbons in pollution: a heart-breaking matter, J. Physiol. 598 (2020) 227, https://doi.org/10.1113/JP278885.

[25] S. Pongpiachan, D. Tipmanee, C. Choochuay, W. Deelaman, N. Iadtem, Q. Wang, L. Xing, G. Li, Y. Han, M.Z. Hashmi, J. Cao, A. Leckngam, S. Poshyachinda, Concentrations and source identification of priority polycyclic aromatic hydrocarbons in sediment cores from south and northeast Thailand, Heliyon 8 (2022) 10953, https://doi.org/10.1016/J.HELIYON.2022.E10953.

[26] B. Yang, L. Zhou, N. Xue, F. Li, Y. Li, R.D. Vogt, X. Cong, Y. Yan, B. Liu, Source apportionment of polycyclic aromatic hydrocarbons in soils of Huanghuai Plain, China: comparison of three receptor models, Sci. Total Environ. 443 (2013) 31–39, https://doi.org/10.1016/J.SCITOTENV.2012.10.094.

[27] A.O. Adegunwa, J.A.O. Oyekunle, O.T. Ore, Distribution and source apportionment of polycyclic aromatic hydrocarbons in indoor dust of an emerging residential city in Nigeria: implication on human health, Environ. Poll. Manag. 2 (2025) 14–22, https://doi.org/10.1016/J.EPM.2025.01.001.

[28] I.A. Bertinetti, C.D. Ferreira, J.L.F. Monks, P.J. Sanches-Filho, M.C. Elias, Accumulation of polycyclic aromatic hydrocarbons (PAHs) in rice subjected to drying with different fuels plus temperature, industrial processes and cooking, J. Food Compos. Anal. 66 (2018) 109–115, https://doi.org/10.1016/J.JFCA.2017.12.009.

[29] M. Sánchez-Guerra, N. Pelallo-Martínez, F. Díaz-Barriga, S.J. Rothenberg, L. Hernández-Cadena, S. Faugeron, L.F. Oropeza-Hernández, M. Guaderrama-Díaz, B. Quintanilla-Vega, Environmental polycyclic aromatic hydrocarbon (PAH) exposure and DNA damage in Mexican children, Mutat. Res., Genet. Toxicol. Environ. Mutagen. 742 (2012) 66–71, https://doi.org/10.1016/J.MRGENTOX.2011.12.006.

[30] L. Tang, P. Wang, C. Yu, N. Jiang, J. Hou, J. Cui, S. Xin, Y. Xin, M. Li, Adsorption of polycyclic aromatic hydrocarbons (PAHs) in soil and water on pyrochars: a review, J. Environ. Chem. Eng. 13 (2025) 116081, https://doi.org/10.1016/J.JECE.2025.116081.

[31] J. Hu, J. Chen, W. Wang, L. Zhu, Mechanism of growth inhibition mediated by disorder of chlorophyll metabolism in rice (Oryza sativa) under the stress of three polycyclic aromatic hydrocarbons, Chemosphere 329 (2023) 138554, https://doi.org/10.1016/J.CHEMOSPHERE.2023.138554.

[32] Y. Li, L. Long, J. Ge, L. xuan Yang, J. jin Cheng, L. xiang Sun, C. Lu, X. yang Yu, Presence, distribution and risk assessment of polycyclic aromatic hydrocarbons in rice-wheat continuous cropping soils close to five industrial parks of Suzhou, China, Chemosphere 184 (2017) 753–761, https://doi.org/10.1016/J.CHEMOSPHERE.2017.06.055.

[33] H.G. Moon, S. Bae, Y. Chae, Y.J. Kim, H.M. Kim, M. Song, M.S. Bae, C.H. Lee, T. Ha, J.S. Seo, S. Kim, Assessment of potential ecological risk for polycyclic aromatic hydrocarbons in urban soils with high level of atmospheric particulate matter concentration, Ecotoxicol. Environ. Saf. 272 (2024) 116014, https://doi.org/10.1016/J.ECOENV.2024.116014.

[34] J. Angulo-Cuero, M.T. Grassi, R.G. Dolatto, A.M. Palacio-Cortés, M. Rosero-Moreano, B.H. Aristizábal, Impact of polycyclic aromatic hydrocarbons in mangroves from the Colombian pacific coast: evaluation in sediments and bivalves, Mar. Pollut. Bull. 172 (2021) 112828, https://doi.org/10.1016/J.MARPOLBUL.2021.112828.

[35] Y. Yan, K. Bao, K. Zhao, B. Neupane, C. Gao, A baseline study of polycyclic aromatic hydrocarbons distribution, source and ecological risk in Zhanjiang mangrove wetlands, South China, Ecotoxicol. Environ. Saf. 249 (2023) 114437, https://doi.org/10.1016/J.ECOENV.2022.114437.

[36] X. Jin, Z. Li, H. Feng, X. Xu, G. Yang, Newly combined spectral indices to improve estimation of total leaf chlorophyll content in cotton, IEEE J. Sel. Top. Appl. Earth Obs. Rem. Sens. 7 (2014) 4589–4600, https://doi.org/10.1109/JSTARS.2014.2360069.

[37] L. Molina, A. Segura, L. Molina, A. Segura, Biochemical and metabolic plant responses toward polycyclic aromatic hydrocarbons and heavy metals present in atmospheric pollution, Plants 10 (2021), https://doi.org/10.3390/PLANTS10112305, 10 (2021).

[38] S. Wu, E. Wu, L. Qiu, W. Zhong, J. Chen, Effects of phenanthrene on the mortality, growth, and anti-oxidant system of earthworms (Eisenia fetida) under laboratory conditions, Chemosphere 83 (2011) 429–434, https://doi.org/10.1016/J.CHEMOSPHERE.2010.12.082.

[39] E.S. Okwute, Z. Mohammed, D.E. Arthur, H. Wayar, J.C. Akan, Assessment of the levels of polycyclic aromatic hydrocarbons (PAHs) in soil and selected vegetable samples from challawa agricultural location in Kano State, Nigeria, Environ. Poll. Manag. 2 (2025) 23–31, https://doi.org/10.1016/J.EPM.2024.12.002.

[40] Z. Liu, X. Li, L. Xu, S. Shuang, Z. Li, Risk assessment of polycyclic aromatic hydrocarbons in the shenfu irrigation area in China and their application for determining the optimum land use model, Soil Sediment Contam. 23 (2014) 464–479, https://doi.org/10.1080/15320383.2014.839624.

[41] Canadian Council of Ministers of the Environment, Canadian soil quality guidelines for carcinogenic and other polycyclic aromatic hydrocarbons, Environ. Human Health Effect) (2010). https://ccme.ca/en/resources. (Accessed 3 September 2025).

[42] Ministerio del Ambiente [MINAM], Decreto Supremo N.° 011-2017-MINAM, Perú, 2017. https://www.gob.pe/institucion/minam/normas-legales/3693-011-2017-minam. (Accessed 14 September 2025).

[43] D. Li, P. Su, M. Tang, G. Zhang, Biochar alters the persistence of PAHs in soils by affecting soil physicochemical properties and microbial diversity: a meta-analysis, Ecotoxicol. Environ. Saf. 266 (2023) 115589, https://doi.org/10.1016/J.ECOENV.2023.115589.

[44] Y. Zhang, K. Meliefste, W. Hu, L. Portengen, N. Rothman, B. Reiss, J. Li, J. Xu, B. Ning, D. Liu, F.R. Cassee, J.Y.Y. Wong, R. Vermeulen, Q. Lan, G.S. Downward, Expanded PAH analysis of household air pollution in a rural region of China with high lung cancer incidence, Environ. Pollut. 361 (2024) 124717, https://doi.org/10.1016/J.ENVPOL.2024.124717.

[45] I.C.T. Nisbet, P.K. LaGoy, Toxic equivalency factors (TEFs) for polycyclic aromatic hydrocarbons (PAHs), Regul. Toxicol. Pharmacol. 16 (1992) 290–300, https://doi.org/10.1016/0273-2300(92)90009-X.

[46] S. Orecchio, F. Bianchini, R. Bonsignore, P. Blandino, S. Barreca, D. Amorello, Profiles and sources of PAHs in sediments from an open-pit mining area in the

Peruvian andes, Polycycl. Aromat. Compd. 36 (2016) 429–451, https://doi.org/10.1080/10406638.2015.1005242.
[47] A. Rosell-Melé, N. Moraleda-Cibrián, M. Cartró-Sabaté, F. Colomer-Ventura, P. Mayor, M. Orta-Martínez, Oil pollution in soils and sediments from the Northern Peruvian Amazon, Sci. Total Environ. (2018) 1010–1019, https://doi.org/10.1016/J.SCITOTENV.2017.07.208, 610–611.
[48] L. Visitación Figueroa, Degradación de hidrocarburos aromáticos policíclicos en residuos de barrido de calles del centro de Lima. Evaluación Del Riesgo Tóxico y Ecotoxicológico, 2016.
[49] A.P. Vega Quispe, D.E. Merma Chacca, I. Maldonado, E.J. Colque Ayma, L. R. Guimarães Guilherme, P.A. Jiménez Jiménez, M.R. Rivera Campano, J.L. Ramos Tejeda, F. Zirena Vilca, Presence and leaching of PAHs in soils of high Andean grasslands affected by intentional burning, Environ. Nanotechnol. Monit. Manag. 21 (2024) 100915, https://doi.org/10.1016/J.ENMM.2024.100915.
[50] E. Tarrillo, M. Arce-Inga, P.A. Torres-Herrera, D. Tineo, V.H. Taboada-Mitma, J. Cruz-Luis, N.B. Rojas-Briceño, N. Atalaya-Marin, D. Gómez-Fernández, M. Goñas, Geospatial distribution of heavy metals in rice soils of northwestern Peru, Sci. Rep. 15 (1) (2025) 30692, https://doi.org/10.1038/s41598-025-16638-6, 15 (2025).
[51] Servicio Nacional de Meteorología e Hidrología [SENAMHI], Climas del Perú - Mapa de Clasifiación Climática Nacional. https://www.senamhi.gob.pe/?p=mapa-climatico-del-peru, 2021. (Accessed 11 January 2025).
[52] M.B. López-Hernández, C. López-Castañeda, J. Kohashi-Shibata, S. Miranda-Colín, E.J. Barrios-Gómez, C.G. Martínez-Rueda, Grain yield and its components, and root density in rice under irrigation and rainfed conditions. https://www.scielo.org.mx/scielo.php?pid=S1405-31952018000400563&script=sci_arttext&tlng=en, 2018. (Accessed 24 December 2025).
[53] Ministerio de Desarrollo Agrario y Riego [MIDAGRI], Superficie Agrícola del Perú. https://siea.midagri.gob.pe/portal/informativos/superficie-agricola-peruana, 2025. (Accessed 16 August 2025).
[54] National Aeronautics and Space Administration [NASA], ASF data search vertex. https://search.asf.alaska.edu/#/, 2025. (Accessed 14 September 2025).
[55] B. Maliszewska-Kordybach, B. Smreczak, A. Klimkowicz-Pawlas, H. Terelak, Monitoring of the total content of polycyclic aromatic hydrocarbons (PAHs) in arable soils in Poland, Chemosphere 73 (2008) 1284–1291, https://doi.org/10.1016/J.CHEMOSPHERE.2008.07.009.
[56] Y. Marusenko, P. Herckes, S.J. Hall, Distribution of polycyclic aromatic hydrocarbons in soils of an arid urban ecosystem, Water Air Soil Pollut. 219 (2011) 473–487, https://doi.org/10.1007/S11270-010-0721-5/FIGURES/5.
[57] K. Wang, Y. Shen, S. Zhang, Y. Ye, Q. Shen, J. Hu, X. Wang, Application of spatial analysis and multivariate analysis techniques in distribution and source study of polycyclic aromatic hydrocarbons in the topsoil of Beijing, China, Environ. Geol. 56 (2009) 1041–1050, https://doi.org/10.1007/S00254-008-1204-5/FIGURES/5.
[58] E.R. Long, D.D. MacDonald, C.G. Severn, C.B. Hong, Classifying probabilities of acute toxicity in marine sediments with empirically derived sediment quality guidelines, Environ. Toxicol. Chem. 19 (2000) 2598–2601, https://doi.org/10.1002/ETC.5620191028.
[59] R.C. Swartz, Consensus sediment quality guidelines for polycyclic aromatic hydrocarbon mixtures, Environ. Toxicol. Chem. 18 (1999) 780–787, https://doi.org/10.1002/ETC.5620180426.
[60] H.T. Workneh, X. Chen, Y. Ma, E. Bayable, A. Dash, Comparison of IDW, Kriging and orographic based linear interpolations of rainfall in six rainfall regimes of Ethiopia, J. Hydrol. Reg. Stud. 52 (2024) 101696, https://doi.org/10.1016/J.EJRH.2024.101696.
[61] P. Zhang, Y. Chen, Polycyclic aromatic hydrocarbons contamination in surface soil of China: a review, Sci. Total Environ. 605–606 (2017) 1011–1020, https://doi.org/10.1016/J.SCITOTENV.2017.06.247.
[62] R.K. Singh, S.K. Singh, Persistent polycyclic aromatic hydrocarbons (PAHs) in the soil, its bioremediation, and health effects, Environ. Sci. Eur. 37 (2025), https://doi.org/10.1186/s12302-025-01230-6.
[63] K.A. Adamson, S. Prion, Making sense of methods and measurement: statistical power, Clin. Simul. Nurs. 9 (2013) e477–e478, https://doi.org/10.1016/J.ECNS.2013.03.002.
[64] X. Ma, C. Huang, Y. Li, S. Li, Q. Jiang, C. Zhang, B. Xue, H. Yang, Influencing factors and risk assessment of polycyclic aromatic hydrocarbons in the sediments of Beilianchi Lake, China, Sci. Total Environ. 981 (2025) 179607, https://doi.org/10.1016/J.SCITOTENV.2025.179607.
[65] V.K. Akinpelumi, K.G. Kumi, A.P. Onyena, K. Sam, A.N. Ezejiofor, C. Frazzoli, O. C. Ekhator, G.J. Udom, O.E. Orisakwe, A comparative study of the impacts of polycyclic aromatic hydrocarbons in water and soils in Nigeria and Ghana: towards a framework for public health protection, J. Hazard. Mater. Adv. 11 (2023) 100336, https://doi.org/10.1016/J.HAZADV.2023.100336.
[66] K. Hui, B. Kou, Y. Jiang, Y. Wu, Q. Xu, W. Tan, Nitrogen addition increases the ecological and human health risks of PAHs in different fractions of soil in sewage-irrigated area, Sci. Total Environ. 811 (2022) 151420, https://doi.org/10.1016/J.SCITOTENV.2021.151420.
[67] D.S. Parihar, M.K. Narang, B. Dogra, A. Prakash, A. Mahadik, Rice residue burning in Northern India: an assessment of environmental concerns and potential solutions – a review, Environ. Res. Commun. 5 (2023) 062001, https://doi.org/10.1088/2515-7620/ACB6D4.
[68] S. Yi, F. Li, C. Wu, F. Ge, C. Feng, M. Zhang, Y. Liu, H. Lu, Co-transformation of HMs-PAHs in rhizosphere soils and adaptive responses of rhizobacteria during whole growth period of rice (Oryza sativa L.), J. Environ. Sci. 132 (2023) 71–82, https://doi.org/10.1016/J.JES.2022.07.017.
[69] J. Cai, X. Wu, J. Yang, Y. Ma, B. Sun, F. Wu, Does higher ratio of wheat straw addition decrease PAHs degradation in PAHs-contaminated paddy soils and PAHs concentrations in rice? Sci. Total Environ. 954 (2024) 176533 https://doi.org/10.1016/J.SCITOTENV.2024.176533.
[70] Z. Sun, Y. Zhu, S. Zhuo, W. Liu, E.Y. Zeng, X. Wang, B. Xing, S. Tao, Occurrence of nitro- and oxy-PAHs in agricultural soils in eastern China and excess lifetime cancer risks from human exposure through soil ingestion, Environ. Int. 108 (2017) 261–270, https://doi.org/10.1016/J.ENVINT.2017.09.001.
[71] A.C. Rencher, G.B. Schaalje, Analysis-of-Variance: the cell means model for unbalanced data, Linear Models Statist. (2007) 413–442, https://doi.org/10.1002/9780470192610.CH15.
[72] A. Andreella, J. Goeman, J. Hemerik, L. Finos, Robust inference for generalized linear mixed models: a "Two-Stage Summary Statistics" approach based on score sign flipping, Psychometrika 90 (2025) 531–553, https://doi.org/10.1017/PSY.2024.22.
[73] H. Bao, S. Hou, H. Niu, K. Tian, X. Liu, F. Wu, Status, sources, and risk assessment of polycyclic aromatic hydrocarbons in urban soils of Xi'an, China, Environ. Sci. Pollut. Control Ser. 25 (2018) 18947–18959, https://doi.org/10.1007/S11356-018-1928-Z/TABLES/5.
[74] R.M. Harrison, D.I.T. Smith, L. Luhana, Source apportionment of atmospheric polycyclic aromatic hydrocarbons collected from an urban location in Birmingham, U.K, Environ. Sci. Technol. 30 (1996) 825–832, https://doi.org/10.1021/ES950252D.
[75] M.F. Simcik, S.J. Eisenreich, P.J. Lioy, Source apportionment and source/sink relationships of PAHs in the coastal atmosphere of Chicago and Lake Michigan, Atmos. Environ. 33 (1999) 5071–5079, https://doi.org/10.1016/S1352-2310(99)00233-2.
[76] M. Duval, S. Friedlander, Source Resolution of Polycyclic Aromatic Hydrocarbons in the Los Angeles Atmosphere Application of A Chemical, 1982. EPA-600/S2-81-161.
[77] T.T.T. Dong, B.K. Lee, Characteristics, toxicity, and source apportionment of polycylic aromatic hydrocarbons (PAHs) in road dust of Ulsan, Korea, Chemosphere 74 (2009) 1245–1253, https://doi.org/10.1016/J.CHEMOSPHERE.2008.11.035.
[78] J. Sabaté, M. Viñas, A.M. Solanas, Bioavailability assessment and environmental fate of polycyclic aromatic hydrocarbons in biostimulated creosote-contaminated soil, Chemosphere 63 (2006) 1648–1659, https://doi.org/10.1016/J.CHEMOSPHERE.2005.10.020.
[79] Ministerio Del Ambiente [MINAM], Decreto Supremo N.° 004-2017-MINAM, El Peruano, Perú, 2017.
[80] Ministerio Del Ambiente [MINAM], Decreto Supremo N.° 003-2010-MINAM, El Peruano, Perú, 2010.
[81] Ministerio De Agricultura [MA], Decreto Supremo N.° 016-2012-AG, El Peruano, Perú, 2012.
[82] Ministerio De Agricultura y Riego [MIDAGRI], Decreto Supremo N.° 007-2024-MIDAGRI, El Peruano, Perú, 2024.